NATL INST OF STAND & TECH
A11107 390618

NBS
PUBLICATIONS

NBSIR 84-2838

Measurement Techniques for High-Power Semiconductor Materials and Devices: Annual Report, January 1, 1982 to March 31, 1983

U.S. DEPARTMENT OF COMMERCE
National Bureau of Standards
National Engineering Laboratory
Center for Electronics and Electrical Engineering
Semiconductor Materials and Processes Division
Washington, DC 20234

April 1984

Prepared for
Department of Energy
Division of Electric Energy Systems
Washington, DC 20461

QC
100
.U56
84-2333
1984
c 2

NATIONAL BUREAU
OF STANDARDS
LIBRARY
Circ
QC
100
.U56
84-2838
1984
c.2

NBSIR 84-2838

MEASUREMENT TECHNIQUES FOR HIGH-POWER SEMICONDUCTOR MATERIALS AND DEVICES: ANNUAL REPORT, JANUARY 1, 1982 TO MARCH 31, 1983

W. R. Thurber, J. R. Lowney, and W. E. Phillips

U.S. DEPARTMENT OF COMMERCE
National Bureau of Standards
National Engineering Laboratory
Center for Electronics and Electrical Engineering
Semiconductor Materials and Processes Division
Washington, DC 20234

April 1984

Prepared for
Department of Energy
Division of Electric Energy Systems
Washington, DC 20461

U.S. DEPARTMENT OF COMMERCE, Malcolm Baldrige, *Secretary*
NATIONAL BUREAU OF STANDARDS, Ernest Ambler, *Director*

TABLE OF CONTENTS

Page

Abstract 1

1. Introduction and Executive Summary 1

2. Lifetime-Predicting Computer Program (LT1) 2

3. Time Dependence of the Capacitance-Voltage Relationship of a Heavily Platinum-Doped Silicon Diode 3

References 8

Appendix A. "The Relationship Between Deep-Level Measurements and Lifetime in Devices" 9

Appendix B. "Analysis of Nonexponential Transient Capacitance in Silicon Diodes Heavily Doped with Platinum" 14

Appendix C. "Improved Analysis Procedures for Deep-Level Measurements by Transient Capacitance" 20

Appendix D. Details and Listing of Lifetime-Predicting Computer Program 26

LIST OF FIGURES

1. Inverse capacitance squared as a function of reverse voltage for a 0 V trap-filling bias with time as a parameter 5

2. Percent error in the emission rate obtained by the capacitance-ratio method compared with the true emission rate for four different bias voltage sequences 7

PREFACE

This work was conducted as a part of the Semiconductor Technology Program at the National Bureau of Standards (NBS). This program serves to focus NBS research to enhance the performance, interchangeability, and reliability of discrete semiconductor devices and integrated circuits through improvements in measurement technology for use in specifying materials and devices in national and international commerce and for use by industry in controlling device fabrication processes. This research leads to carefully evaluated and well-documented test procedures and associated technology. Special emphasis is placed on the dissemination of the results of the research to the electronics community. Application of these results by industry will contribute to higher yields, lower cost, and higher reliability of semiconductor devices. Improved measurement technology also leads to greater economy in government procurement by providing a common basis for the purchase specifications of government agencies and, in addition, provides a basis for controlled improvements in fabrication processes and in essential device characteristics.

The segment of the Semiconductor Technology Program described in this annual report was supported by the Division of Electric Energy Systems of the Department of Energy (DoE) under NBS/DoE Task Order DE-A101-76PRO6010. The contract was monitored by Mr. Kenneth Klein of DoE. The NBS contacts for technical information on this project are W. R. Thurber and J. R. Lowney of the Semiconductor Materials and Processes Division at the National Bureau of Standards, (301) 921-3625.

The authors would like to acknowledge guidance and support from R. D. Larrabee and other colleagues at the National Bureau of Standards.

Measurement Techniques for High-Power Semiconductor Materials and Devices

ANNUAL REPORT

January 1, 1982 to March 31, 1983

W. R. Thurber, J. R. Lowney, and W. E. Phillips
Semiconductor Materials and Processes Division
National Bureau of Standards
Washington, DC 20234

ABSTRACT

This annual report is the final one in a series which describes NBS research to develop procedures for the effective utilization of deep-level measurements to detect and characterize defects which reduce lifetime or contribute to leakage current in power-device-grade silicon. During this reporting period, the previously written computer program for predicting excess-carrier lifetime was revised to calculate more accurately lifetimes for high or low injection conditions and in space-charge regions. Comparisons were made between lifetime measurements on platinum-doped silicon diodes and the predictions of the computer model. As part of the effort to extend the procedures to analyze data from nonexponential transient capacitance measurements, the time dependence of the capacitance-voltage relationship of a heavily platinum-doped silicon diode was measured as a function of bias voltage. Included as appendices are three recent publications resulting from the work. A listing of the lifetime-predicting computer program is also an appendix.

Key words: deep-level measurements; deep-level transient spectroscopy; defect characterization; lifetime; power-device grade silicon; transient capacitance techniques.

1. INTRODUCTION AND EXECUTIVE SUMMARY

This annual report describes results of NBS research directed toward the development of measurement methods for semiconductor materials and devices which will lead to more effective use of high-power semiconductor devices in applications for energy generation, transmission, conversion, and conservation. The major effort under this program has been to develop procedures for the effective utilization of deep-level measurements to detect and characterize defects which reduce lifetime or contribute to leakage current in silicon used for power devices.

The presence of deep-level impurities in semiconductor power devices is a consequence of their unintentional introduction during crystal growth and during the wafer fabrication procedure or their intentional introduction in order to adjust the switching properties of the device. In either case, the dominant effect of the deep level is to modify the excess-carrier lifetime. Measurement techniques to detect, characterize, and identify such deep levels are required in order to monitor the presence of unintentional contamination and to characterize and understand the behavior of intentionally added impurities. The use of such techniques for process diagnostics would enhance the

manufacturer's ability to control the yield, reliability, and cost of his product.

During the period covered by this report, the previously written computer program for predicting excess-carrier lifetime was revised to calculate lifetimes more accurately for high or low injection conditions and in space-charge regions. The model accepts input parameters, namely, activation energies and capture cross sections, derived from thermal emission-rate measurements on appropriately doped material. Comparisons were made between lifetime measurements on platinum-doped silicon diodes and the predictions of the computer model. Reasonable agreement was obtained in magnitude and temperature dependence for both n- and p-type silicon. The results of this work were presented at the 1983 Custom Integrated Circuits Conference in Rochester, New York. The paper which appeared in the proceedings of the conference is reproduced as Appendix A in this report. A listing of the computer code for the revised lifetime-predicting program is given in Appendix D.

During the previous reporting period, a method was developed to analyze non-exponential capacitance transients. The method was refined during this reporting period and published in the Journal of Applied Physics. The paper is reproduced in Appendix B. The procedures given in the paper were then applied to the more commonly used deep-level transient spectroscopy (DLTS) technique. A talk covering this work was presented at the Electrochemical Society's "Defects in Silicon" symposium held in San Francisco in May 1983. The associated paper was published in the symposium proceedings and is reproduced as Appendix C of this report. As part of the effort to extend the generalized analysis procedures to DLTS, the time dependence of the capacitance-voltage relationship of a heavily platinum-doped silicon diode was measured as a function of bias voltage. Because a description of this work was not included in the published paper, it appears as Section 3 of this report.

In response to a request by the American Society for Testing and Materials (ASTM), a draft document entitled "Standard Practice for Characterizing Semiconductor Deep Levels by Transient Capacitance Techniques" was written and subsequently revised to incorporate suggestions received from ASTM Committee F-1. The latest version of this draft document is available from the authors.

2. LIFETIME-PREDICTING COMPUTER PROGRAM (LT1)

This FORTRAN-77 computer program computes the minority-carrier lifetime in silicon as a function of temperature and injection level. It can handle up to three donor and three acceptor species (including the shallow dopants) which have a single level in the energy gap. Along with these levels, it can handle two multilevel species of the same type as platinum and gold (i.e., having both a donor and acceptor level in the gap). It is assumed that all these centers act independently, and Shockley-Read-Hall theory of recombination through traps can be used to compute the lifetime.

The necessary trap and dopant parameters (density, energy, degeneracy, and cross sections) are inputs to the program. The formulas used for lifetime

prediction are given in references [1] and [2]. It is important to realize that the excess- carrier recombination lifetime varies greatly with injection ratio and computational difficulties may arise if more than one trap is present.

The degeneracy factor g, defined in reference [3], requires a word of explanation. For shallow dopants, it is an integer for both donors (g = 2) and acceptors (g = 4). For traps, it is a positive real number equal to $\exp(\Delta S/k)$, where ΔS is the change in entropy associated with emission of a carrier and k is the Boltzmann constant. It is related to both the electronic degeneracy of the trap as well as any relaxation of the lattice after emission. The physics of the degeneracy factor is described in reference [3]. An alternative method of dealing with the degeneracy factor is to incorporate it into the trap energy, as done in Appendix A. If this method is used, the trap energy is now called the Gibbs free energy, which is equal to $(E_T - T\Delta S)$, where E_T is the energy position of the trap level in the gap and T is absolute temperature.

A discussion of the details of the program, a listing, and sample input and output are given in Appendix D.

3. TIME DEPENDENCE OF THE CAPACITANCE-VOLTAGE RELATIONSHIP OF A HEAVILY PLATINUM-DOPED SILICON DIODE

A method was developed to analyze nonexponential capacitance transients measured under conditions such that the trap density is not small compared with the net shallow dopant density. Charging the traps in only part of the depletion region during the fill pulse is taken into account by the method. For spatially constant trap and shallow dopant densities, partial charging increases the nonexponentiality which would otherwise exist for a given ratio of trap density to shallow dopant density. This capacitance-ratio method was initially developed for isothermal transient capacitance (ITCAP) [4] and was extended to the more commonly used DLTS technique [5]. It is assumed in the approach that there is a nearly linear relationship between C^{-2} and V for the p-n junction test diode. By making the depletion approximation, it is shown that the time dependent density of electrons on the defect centers, n_t, in the depletion region of a p^+n junction under reverse bias V_r is [4]:

$$n_t = N_d - \frac{2(V_r - V_c)C_b^2C^2}{q\varepsilon A^2(C_b^2 - C^2)}, \qquad (1)$$

where C is the junction capacitance, C_b is the capacitance at some reduced trap-filling bias V_c, A is the junction area, ε is the dielectric constant (permittivity) of silicon, N_d is the shallow-dopant density (assumed to be constant), and q is the electronic charge.

However, in order to include the effects related to large ratios of trap to shallow-dopant density, eq (1) was generalized by replacing the number "2" with a dimensionless parameter α which may vary with V_r, V_c, and time. The dependence of α on these quantities is related to the ratio of N_t/N_d, but is very complex. In rearranged form, this new equation is:

$$C^{-2} = C_b^{-2} + \frac{\alpha(V_r - V_c)}{q\varepsilon A^2(N_d - n_t)} . \qquad (2)$$

To examine the relationship in eq (2) as a function of time and voltage, measurements were made on a platinum-doped, n-type silicon diode on wafer 93B (wafer containing device no. 2 in Appendices B and C) at -156°C. The results of C^{-2} *vs.* V_r are shown in figure 1 as a function of reverse bias for a trap-filling bias of 0 V. Points were obtained for four different times: (1) at $t = t_i$ ($C = C_i$), corresponding to restoration of the reverse bias; (2) at $t = t_1$, the first boxcar gate-delay time; (3) at $t = t_2$, the second boxcar gate-delay time; and (4) at $t = t_f$ ($C = C_f$) after the transient has decayed. Even though the present device is from the same wafer as device no. 2, approximate fitting of the C^{-2} *vs.* V_r relationships suggested a trap to shallow dopant density ratio of about 0.5 instead of the 0.38 found for device no. 2. Consequently, the calculated values for n_t in [4] cannot be used for the present diode.

Nonlinear behavior is evident in all four curves in figure 1 at low voltages with the most pronounced curvature occurring for the data obtained at $t = t_i$. Therefore, it may be concluded that α varies with voltage for fixed time. It is impossible to determine *a priori* the variation of α with time from these data and eq (2) because of our lack of knowledge of n_t. However, with certain assumptions, it was possible to obtain information on α from the curves in figure 1. It was assumed that $n_t = N_t e^{-e_n t}$, a good approximation at low temperatures, where N_t is the total trap density, and e_n is the emission rate for electrons. The value of e_n was obtained from a plot of the capacitance ratio for this diode, a technique which is discussed below. First, for $V_r = 10$ V, a value of $\alpha = 2.40$ was calculated from the t_f ($t = \infty$) curve using eq (2) with $N_d = 1.21 \times 10^{15}$ cm^{-3} from reference [4] and the measured C_b. Second, $N_t = 6.1 \times 10^{14}$ cm^{-3} was calculated from the t_2 ($t = 20$ ms) curve using this α. Then, with N_t and N_d known, α was calculated from the t_1 ($t = 10$ ms) curve and found to be in good agreement with the value from the t_f curve where only N_d entered. Keeping these N_t and N_d values, α was also calculated from the t_i ($t = 0$) curve. The value of α was about 4% smaller at t_i than at t_1. This trend agrees with more precise results obtained from idealized data, which will be given later, and shows the need to consider the variation of α with time in our analysis.

It is assumed in the capacitance-ratio method [4,5] that α is constant during the capacitance transient. To obtain the time constant of the transient, a ratio of capacitances C_r is plotted as a function of time. If α changes a significant amount with time, a straight line would not result from the semilogarithmic plot of C_r. However, in the following analysis it will be shown that the capacitance-ratio method is relatively insensitive to moderate changes in α and gives a surprisingly accurate result for the emission rate.

In the capacitance-ratio method

$$e_n^r = -\frac{1}{t} \ln \left\{ \frac{(C_b^2 - C_i^2)(C_f^2 - C^2)}{(C_b^2 - C^2)(C_f^2 - C_i^2)} \right\} \equiv -\frac{\ln(C_r)}{t} . \qquad (3)$$

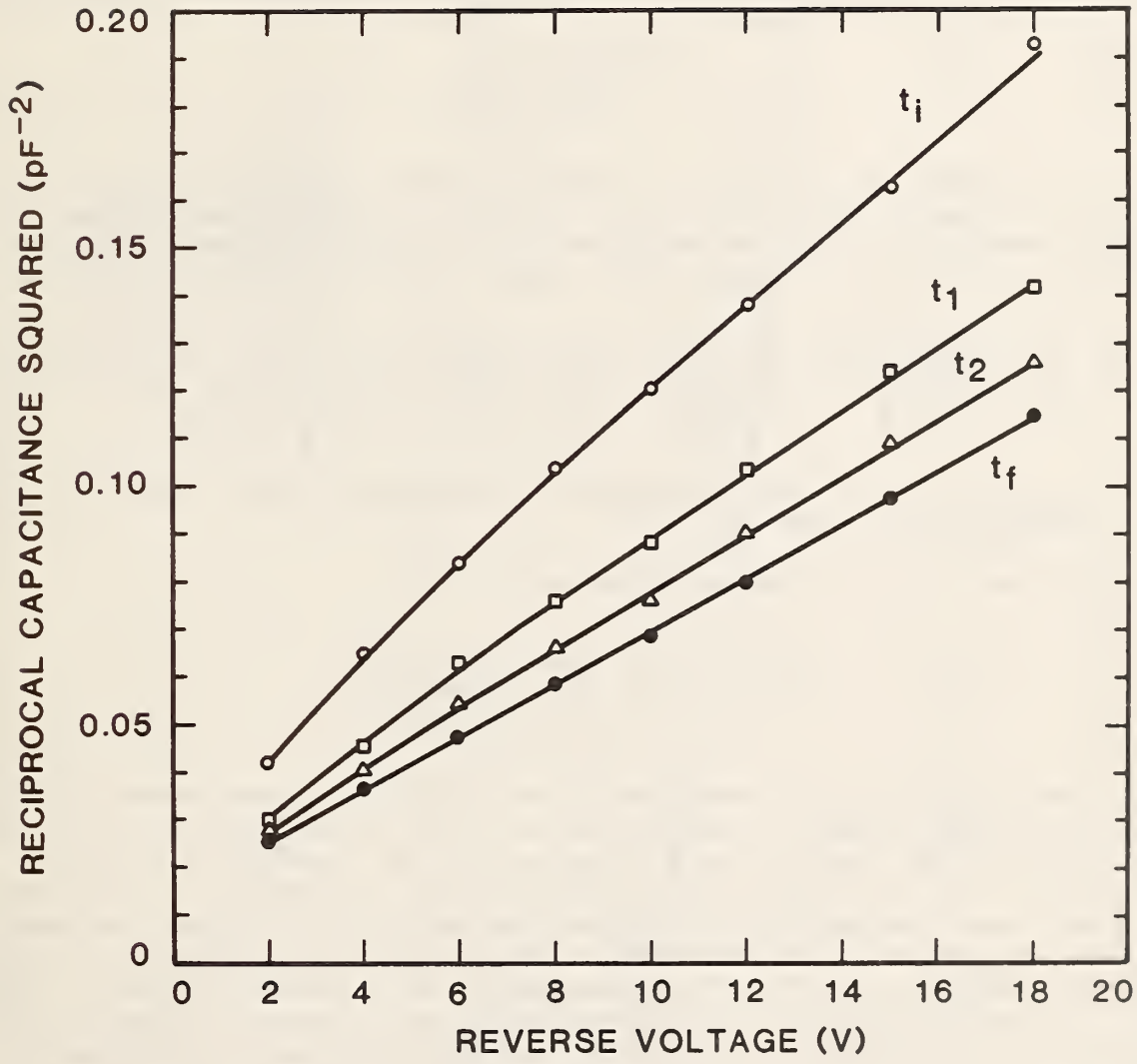

Figure 1. Inverse capacitance squared as a function of reverse voltage for a 0 V trap-filling bias with time as a parameter. The time t_i is when the reverse bias is restored, t_1 is 10 ms later, t_2 is 20 ms after t_i, and t_f is after complete decay of the transient. The measurements were made on a platinum-doped silicon diode on wafer 93B at -156°C. The time constant calculated from the capacitance-ratio method for this family of curves is 15 ms.

The error in the capacitance-ratio method can be expressed as

$$e^{-e_n t} = C_r + C_{err} , \tag{4}$$

where C_{err} is the error which must be added to C_r for a calculation of the true emission rate e_n. This error is obtained by evaluating the expression

$$e^{-e_n t} = \frac{n_t - n_{tf}}{n_{ti} - n_{tf}} , \tag{5}$$

where n_t is given by eq (2), rearranged, and where n_{tf} is the value of n_t at $t = \infty$ and n_{ti} is the value at $t = 0$. C_{err} is the difference between the general case where α is time dependent and the capacitance-ratio version which assumes that α is constant with time. This difference is given by

$$C_{err} = \frac{(C_b^2 - C_i^2)}{(C_b^2 - C^2)} \left[\frac{(\alpha_f - \alpha) C^2 C_f^2 + (\alpha_i - \alpha_f) C_f^2 C_i^2 + (\alpha - \alpha_i) C_i^2 C^2)}{\alpha_f C_f^2 C_b^2 - \alpha_i C_i^2 C_b^2 + (\alpha_i - \alpha_f) C_i^2 C_f^2} \right] , \tag{6}$$

where α is given by eq (2), rearranged, and where α_f is the value of α at $t = \infty$ and α_i is the value at $t = 0$.

The fractional error in the emission rate is

$$\frac{e_n^r - e_n}{e_n} = - \frac{\ell n(1 + C_{err}/C_r)}{\ell n(C_r + C_{err})} . \tag{7}$$

It is not possible to use experimental data directly to determine accurately the error in the emission rate because n_t is not known *a priori* and the deionization of the shallow dopant (discussed in the appendix in ref. [4]) which varies at low temperature is also unknown. Consequently, idealized data were generated using the extended Sah-Reddi model given in the appendix of reference [4] with the parameter values equal to those obtained in reference [4] for device no. 2. The fractional error in emission rates, in percent, is plotted in figure 2 as a function of the product of emission rate and time. At exactly $t = 0$, eq (7) is indeterminate and the error must be evaluated in the limit as t approaches 0. For long times (large $e_n t$) the error goes to zero. It is evident from the trend of the error that it is important to avoid a small value of reverse bias V_r when the fill pulse is near 0 V. Compared with the other voltage sequences, the 5,0,5 V sequence has the largest value of α and the most time-dependent α as calculated from the idealized data using eq (2), rearranged. This is in qualitative agreement with the large change in curvature of the C^{-2} *vs.* V_r plots at low bias voltages in figure 1. Specifically for the 5,0,5 V bias sequence, the change in α between $e_n t = 0$ and $e_n t = 2$, relative to the value at $t = 0$, is 9.3 percent and the error in the emission rate at $e_n t = 1$ is 0.16 percent. For the 5,4,5 V sequence, the corresponding change in α is 6.1 percent and the corresponding error in the emission rate is only 0.08 percent. For the 15,0,15 V

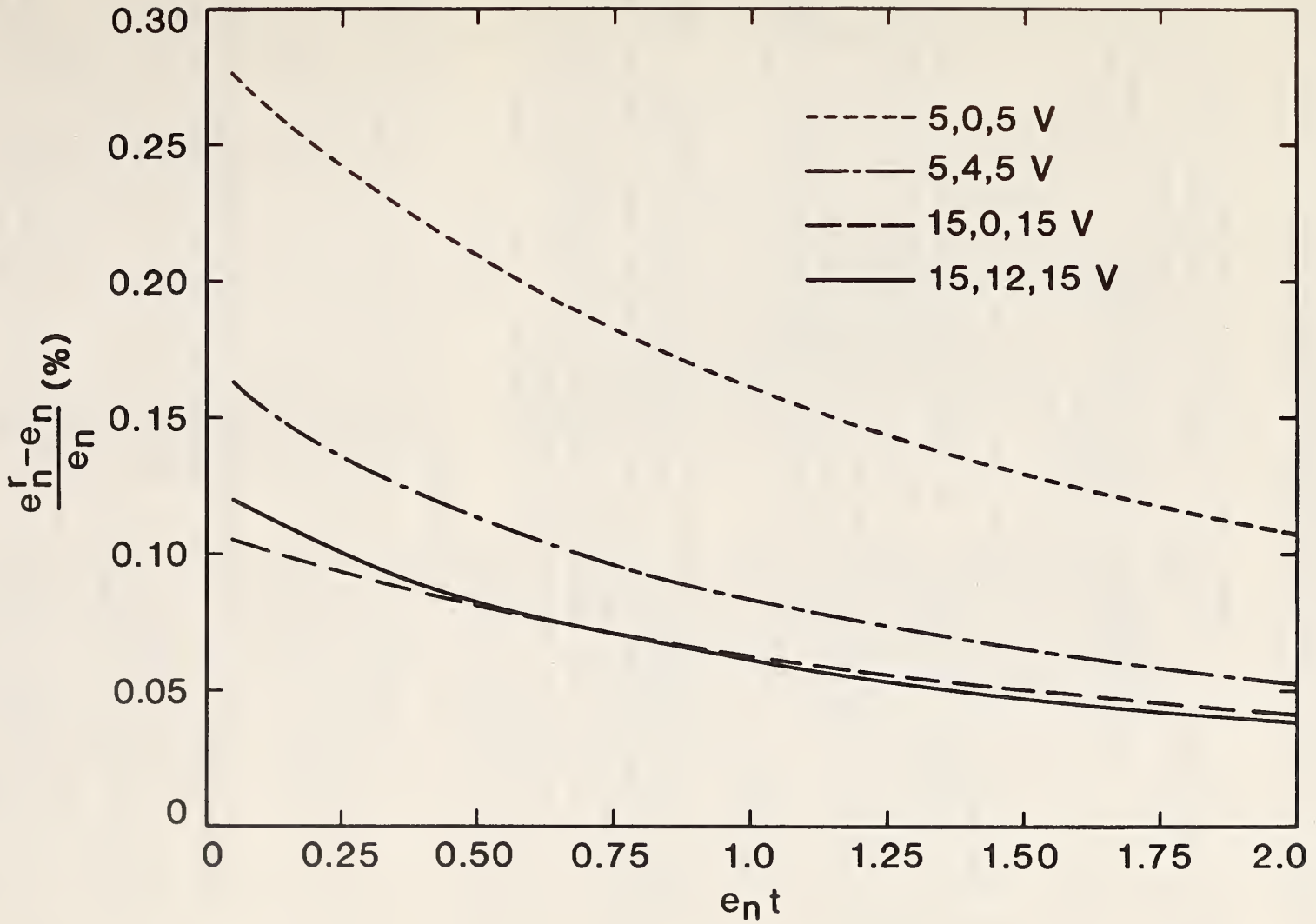

Figure 2. Percent error in the emission rate obtained by the capacitance-ratio method compared with the true emission rate for four different bias voltage sequences. This figure was prepared from idealized data generated using N_t/N_d = 0.38, N_d^+/N_d = 0.77, and T = 87.7 K.

sequence, the relative change in α is 6.5 percent and for the 15,12,15 V sequence, α changes by 3.8 percent. The latter two bias sequences have the same error in emission rate, 0.06 percent at $e_n t = 1$. This is a consequence of the change in α being offset by the effect of C_b in the C_{err} expression, which is larger at 0 V fill-pulse voltage.

While figure 2 shows that a larger reverse voltage is generally desirable, the measured capacitance is consequently smaller, and as a result stray capacitance and noise can have a greater effect on the measurement. Also, one may not want to use a large reverse voltage if the emission rate depends on electric field. A small difference between the reverse- and fill-pulse voltages is especially desirable at low reverse bias voltages to minimize the error in the capacitance-ratio method. However, if the difference is too small, C_i, C_f, C_b, and C are nearly equal so that the results are very sensitive to errors in any of them. Another consideration in minimizing error is to ignore the initial decay of the transient and only analyze data for which $e_n t > 0.5$, for example. In general, the capacitance-ratio method is sufficiently accurate at all times (except for $t \ll 1/e_n$) to justify its use as a convenient way to correct for a large relative trap density and for incomplete trap filling in the depletion region. The latter effect occurs in capacitance *vs.* voltage depth profiling and other applications where a small voltage difference is used. Since we have not considered gradients in trap concentration, however, a more complete analysis would be necessary for profiling experiments.

The DLTS adaptation of the capacitance-ratio method was experimentally demonstrated in the paper in Appendix C. In that work data were collected with two voltage sequences and two boxcar gate-time ratios for each sequence. The emission rates obtained from the analysis procedure were essentially identical for the smaller gate-time ratio, but were slightly different for the larger ratio. This kind of experimental verification, that the emission rate is independent of changes in experimental parameters, should be done in any use of the capacitance-ratio method.

REFERENCES

1. Ghandhi, S. K., *Semiconductor Power Devices: Physics of Operation and Fabrication Technology* (Wiley & Sons, New York, 1977), pp. 2-31.

2. Moll, J. L., *Physics of Semiconductors* (McGraw-Hill, New York, 1964), pp. 92-101.

3. Engstrom, O., and Alm, A., Thermodynamical Analysis of Optimal Recombination Centers in Thyristors, *Solid-State Electronics* 21, 1571-1576 (1978).

4. Phillips, W. E., and Lowney, J. R., Analysis of Nonexponential Transient Capacitance in Silicon Diodes Heavily Doped with Platinum, *J. Appl. Phys.* 54, 2786-2791 (1983) [in Appendix B].

5. Phillips, W. E., Thurber, W. R., and Lowney, J. R., Improved Analysis Procedures for Deep-Level Measurements by Transient Capacitance, *Defects in Silicon*, Proc. Vol. 83-9, W. M. Bullis and L. C. Kimerling, Eds. (Electrochemical Society, Princeton, N. J., 1983), pp. 485-490 [in Appendix C].

APPENDIX A

Reprinted from IEEE PROCEEDINGS OF THE
CUSTOM INTEGRATED CIRCUITS CONFERENCE, May 1983

THE RELATIONSHIP BETWEEN DEEP-LEVEL MEASUREMENTS AND LIFETIME IN DEVICES*

Jeremiah R. Lowney, Robert D. Larrabee, and W. Robert Thurber

Semiconductor Materials and Processes Division
National Bureau of Standards
Washington, DC 20234

Abstract

The minority-carrier lifetime in silicon devices affects performance by influencing such lifetime-related quantities as switching times, storage times, and reverse-leakage currents. A computer program has been developed to model the behavior of deep-level recombination centers that control the minority-carrier lifetime. The input parameters that characterize the deep levels can be measured by capacitive-transient techniques coupled with a measurement of the low-injection-level lifetime. These parameters can be used for deep-level identification and diagnostic purposes and, as input to the program, for predicting lifetime under different injection-level conditions. This technique of deep-level characterization is illustrated for n^+p and p^+n diodes containing deep levels from intentionally added platinum.

I. Introduction

Recombination and thermal generation of carriers can be important in limiting and controlling the behavior of silicon devices and integrated circuits. The minority-carrier lifetime in the base and emitter of bipolar devices can limit their gain. Generation (reverse leakage) currents in charge-storage devices (e.g., CCDs and dynamic RAMs) adversely affect their refresh times. The needed switching speeds of some high-speed logic circuits and high-power devices require intentionally added recombination centers to provide the required rapid response (e.g., TTL logic circuits). Therefore, there is a need for a thorough understanding of the theory of carrier recombination and of thermal generation and its relation to the diagnostic techniques used to characterize deep levels which control this behavior. We consider the Shockley-Read-Hall (SRH) theory[1] of recombination/generation through deep-level traps and, in particular, the expressions for the high-level, low-level, and space-charge recombination lifetimes.[2] We then relate the parameters of this model to the quantities measured by deep-level transient spectroscopy (DLTS)[3] and by low-injection-level lifetime measurements. In this way, deep-level characterization parameters are obtained for identification and diagnostic purposes, for modeling device behavior, and for predicting lifetime under different injection-level conditions.

The analysis procedure developed in this paper is illustrated by application to n^+p and p^+n diodes containing deep levels produced by intentional platinum doping. The minority-carrier capture cross sections obtained in this way are compared to the results obtained by other techniques. The practicality of DLTS measurements on production-line material is demonstrated by results for a commercially available high-voltage rectifier diode.

II. Theory

The Shockley-Read-Hall (SRH)[1] theory of recombination through deep-level traps gives the following expression for the steady-state recombination of electrons and holes, -U, through a single-level trap:[2]

$$-U \equiv \frac{-dp}{dt} = \frac{-dn}{dt} = \frac{(pn-n_i^2)}{(n+n_1)\tau_{po}+(p+p_1)\tau_{no}} , \quad (1)$$

where n and p are the total electron and hole densities,

$$\tau_{no} = (N_T v_t \sigma_n)^{-1} , \quad (2)$$

$$\tau_{po} = (N_T v_t \sigma_p)^{-1} , \quad (3)$$

$$n_1 = N_c \exp[(G_T - E_c)/kT] , \text{ and} \quad (4)$$

$$p_1 = N_v \exp[(E_v - G_T)/kT] . \quad (5)$$

In these expressions N_T is the trap concentration, v_t is the thermal velocity of the carrier, $\sigma_{n,p}$

*This work was conducted as part of the Semiconductor Technology Program at NBS and was supported in part by the Division of Electric Energy Systems, Department of Energy (Task Order A021-EES). Contribution of the National Bureau of Standards, not subject to copyright.

are the carrier capture cross sections, $N_{c,v}$ are the densities of states in the bands, $E_{c,v}$ are the band-edge energies, G_T is the Gibbs free energy of the trap, k is Boltzmann's constant, and T is absolute temperature.

The minority-carrier recombination lifetime τ may be obtained from eq (1):

$$\tau_p \equiv \frac{-p'}{U} = \tau_{po} \frac{(n_0+n_1+n')}{(n_0+p_0+n')} + \tau_{no} \frac{(p_0+p_1+n')}{(n_0+p_0+n')} , \quad (6)$$

where the semiconductor is assumed to be n-type, n_0 and p_0 are, respectively, the equilibrium electron and hole concentrations and n' = p', the excess carrier concentrations. It is very important to realize that the lifetime is a function of the injection ratio, p'/n_0, and this ratio should be measured as part of any lifetime measurement. For $p' << n_0$, τ_p is the low-level lifetime given by:

$$\tau_p^{LL} = \tau_{po} \frac{(n_0+n_1)}{(n_0+p_0)} + \tau_{no} \frac{(p_0+p_1)}{(n_0+p_0)} . \quad (7)$$

If $n' >> n_0$, τ_p is the high-level lifetime given by:

$$\tau_p^{HL} = \tau_{po} + \tau_{no} . \quad (8)$$

At intermediate values of p', the lifetime is not easily measured since it varies as the excess-carrier density decays. It should be noted that only in the limits of high- and low-injection level is the lifetime measured by the transient decay of minority carriers described by eq (6). At intermediate injection levels, the trap occupancies may vary during the transient.

The thermal generation rate in a space-charge region may also be computed from eq (1):

$$U = n_i^2/(n_1\tau_{po}+p_1\tau_{no}) \equiv n_i/(2\tau^{SC}) , \quad (9)$$

where τ^{SC} is called the space-charge generation lifetime. It is important to recognize that these three lifetimes (i.e., τ^{SC}, τ^{LL}, and τ^{HL}) can be very different in value. A center which may not contribute substantially to recombination in the quasi-neutral region of a device may dominate in the space-charge regions because it has a near mid-gap value of free energy. Because different centers may contribute to different lifetimes, a fully characterized model that can include all the recombination centers in the material is required.

We focus now on the low-level lifetime in n-type material since it is usually straightforward to measure on a device by reverse-recovery[4] or by open-circuit-voltage-decay[5] techniques. At low temperatures, n_1, p_1, and p_o are negligible and $\tau_p^{LL} = \tau_{po}$, a quantity which is usually not strongly dependent on temperature. For deep acceptor levels (electron traps) one obtains $\tau_p^{LL} \approx \tau_{po}(1 + n_1/n_o)$ as temperature increases somewhat, but before p_1 and p_o become significant. Correspondingly, for deep donor levels (hole traps), one obtains $\tau_p^{LL} \approx \tau_{po} + \tau_{no}(p_1/n_o)$. Midgap levels would obey $\tau_p^{LL} \approx \tau_{po}(1 + n_1/n_o) + \tau_{no}(p_1/n_o)$ as long as $p_o << n_o$. (Shallow levels are generally not efficient recombination centers because of their small minority-carrier capture cross sections.) These three cases must be distinguished and the pertinent parameters measured in order to apply a model of the lifetime to actual devices. A very accurate method for doing this is deep-level transient spectroscopy (DLTS).

The methods of capacitance transient spectroscopy[6] and DLTS,[3] in particular, furnish information regarding the energy, density, and capture cross sections of deep levels. In DLTS, the high-frequency ($\approx$1 MHz) capacitance of a test p-n junction under reverse bias is measured at two selected times, t_1 and t_2, following a trap-filling period of reduced bias. After trap filling, the reverse bias is restored, and the traps in the space-charge region thermally emit their trapped carriers. This changes the bulk space-charge density in the depletion region and thus changes the junction capacitance. Measuring the difference in capacitance at two selected times during the transient provides a convenient way to characterize this exponential decay and to produce a signature for any deep level because this response will peak at a reproducible temperature for any given values of the times at which the capacitance is measured. The emission rate, e, (reciprocal response time) at the temperature of the peak response is given by:

$$e = \frac{\ln (t_2/t_1)}{t_2-t_1} . \quad (10)$$

Theoretically, this emission rate for electrons is given by:[7]

$$e_n = \sigma_n v_t N_c \exp(-G_T/kT) . \quad (11)$$

All the quantities of eq (11) are, in general, a function of temperature except Boltzmann's constant. It is very important to recognize that G_T is the Gibbs free energy of the trap and not the difference in energy between the trap and the conduction band edge. It is the Gibbs free energy which is needed in the recombination eqs (4) and (5), so eq (11) can be used to derive a value for G_T. However, the majority-carrier capture cross section, $\sigma_n(T)$, is an unknown function of temperature. Thus, an independent measurement of $\sigma_n(T)$ is necessary at each temperature, particularly at the cryogenic temperatures where emission rates are often measured.

A method for measuring the majority-carrier capture cross sections has been discussed by Brotherton *et al.*[8] The change in charge on the traps is measured as a function of filling time by determining the change in applied bias needed to maintain a constant high-frequency capacitance after the filling pulse is removed. A feedback system capable of measuring capacitance in times of the order of a microsecond is needed. If the cross section is not measured independently and customary Arrhenius plots[3] are made to determine the activation energy from eq (10), it is impor-

tant to remember that the energy obtained is not the Gibbs free energy needed for lifetime modeling and is, in general, only a signature of the emission process of the trap. Even if the cross section is temperature independent and the temperature dependencies of v_t and N_c are taken into account, an Arrhenius plot will not, in general, yield G_T because G_T is itself temperature dependent. However, a characteristic signature of the deep level can often be obtained in this way.

Another needed parameter is the minority-carrier capture cross section. Various techniques[9,10] have been described to measure this parameter in a manner similar to that of the majority-carrier cross section. However, the need to generate minority carriers either by injection from a second p-n junction[9] (transistor) or by illumination[10] makes such measurements very difficult. In addition, there are difficulties in measuring the minority-carrier density that is so generated. The approach used in this paper is to use the measured low-level lifetime to determine this cross section. This necessitates modeling the SRH recombination kinetics on a computer and fitting the low-injection-level lifetime vs temperature to the model using measured values for all parameters except the minority-carrier capture cross section. This requires knowledge of the trap density, N_T, which can be determined from the amplitude of the capacitance transient in DLTS or other capacitance transient measurements.[3]

III. Applications

As an example of the above technique, we have considered the case of platinum in silicon. A computer program was written to evaluate the equilibrium carrier density and lifetime expressions as a function of both temperature and injection ratio. Since Pt-doped silicon is thought to have both a deep-acceptor and a deep-donor level associated with each center, multi-level trap statistics were used. The generalization of eq (1) for Pt is:[11]

$$-dn/dt = \frac{(pn-n_i^2)(n_{1A}\tau_{pA}+p\tau_{nA}+p_{1D}\tau_{nD}+n\tau_{pD})}{T_1+T_2+T_3} \qquad (12)$$

where

$$T_1 = (p\tau_{nD}+n_{1D}\tau_{pD})(p\tau_{nA}+n_{1A}\tau_{pA}) \qquad (13)$$

$$T_2 = (n\tau_{pD}+p_{1D}\tau_{nD})(p\tau_{nA}+n_{1A}\tau_{pA}) \qquad (14)$$

$$T_3 = (n\tau_{pD}+p_{1D}\tau_{nD})(n\tau_{pA}+p_{1A}\tau_{nA}) \qquad (15)$$

where the meanings of terms are the same as in eq (1) except that subscripts "D" and "A" have been added to denote the deep donor and deep acceptor level.

The needed parameters, except for minority-carrier capture cross sections, have been taken from Brotherton's work on the Pt impurity center:[12] $E_{TA} = E_c - 0.231 - kT \ln(0.5)$, $E_{TD} = E_v + 0.314 - kT \ln(3.7)$, $\sigma_{nA} = 7.0 \times 10^{-15}$ cm^2, and $\sigma_{pD} = 8 \times 10^{-16}$ cm^2. These values do not contain any temperature dependences since their exact variations are still in question. For our purposes, these cross sections should be adequate since we are going to fit lifetime data that are measured at temperatures greater than 200 K. At these temperatures the cross sections are expected to be relatively constant, having values close to those given above. The lifetime data were taken from Miller *et al.*[13] The reverse-recovery method used by Miller is expected to yield the low-level lifetime although this is not confirmed in their paper. The trap densities used were based on the results of the curve fitting that they performed on their N_T data (measured by thermally stimulated current techniques for four cases: 2.0×10^{13}, 7.0×10^{13}, 2.1×10^{14}, and 6.0×10^{14} cm^{-3} at Pt-diffusion temperatures of 850, 900, 950, and 1000°C, respectively.

The results of our fitting their lifetime data are shown in figures 1 and 2. The minority-carrier cross section so obtained for n-type material (2×10^{-14} cm^2) agrees with measurements by Brotherton,[9] but the minority-carrier capture cross section for p-type material (2×10^{-14} cm^2) is a factor of four higher than Brotherton's value.[9] We are not certain whether Brotherton's measured cross section is accurate for p-type material because of the difficulty in measuring minority cross sections by transient capacitance techniques, or whether the trap density is not the same in p-type and n-type material. Only p^+n diodes were used to determine N_T in the work of Miller *et al.*[13] so it is impossible to determine which of the above possibilities is correct.

The overall agreement between their data and our computation is shown in figures 1 and 2. At low temperatures, the measured lifetime values are generally below our fitted curves, especially for the more lightly Pt-doped cases. This deviation is attributed to the presence of another presumably very deep trap in their specimens which preferentially reduces the lifetime at low temperatures. In their fits to the data, Miller *et al.* used a simplified SRH-based model, which neglected the terms containing the majority cross sections. These terms are included in the present model, and therefore, their derived minority cross sections differ significantly from ours.

Our model now furnishes us the ability to predict the high-level and space-charge-generation lifetimes. The values for the high-level, and especially the space-charge generation lifetimes, differ considerably from the low-level values. At room temperature in n-type silicon, with a Pt-diffusion temperature of 1000°C, the high-level lifetime was calculated to be 26 ns and the space-charge lifetime was calculated to be 100 μs as compared with a low-level lifetime of 14 ns. The situation is similar in p-type silicon for which $\tau^{HL} = 26$ ns, $\tau^{SC} = 100$ μs, and $\tau_n^{LL} = 8$ ns. In practice, the space-charge lifetime may differ somewhat from these calculated values because of high-electric-field effects in the space-charge region.[9]

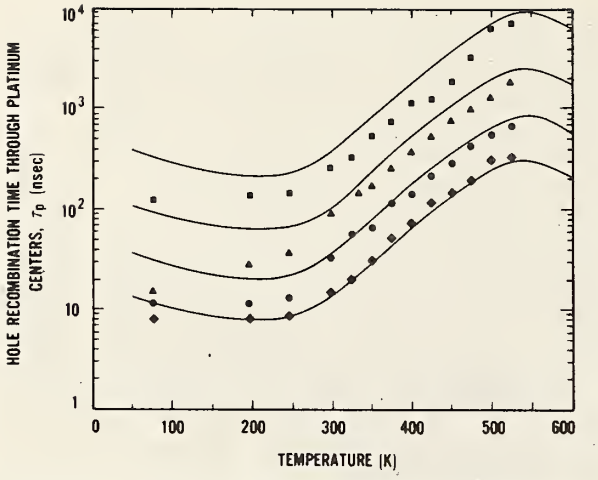

Figure 1. Hole recombination times through the platinum center in 2 Ω•cm n-type silicon as a function of temperature. The solid lines represent lifetimes calculated according to eq (12), and the data points are measured lifetimes from ref. 13 for four p^+n diodes diffused with Pt. The diffusion temperatures are: ■, 850°C; ▲, 900°C; ●, 950°C; and ◆, 1000°C.

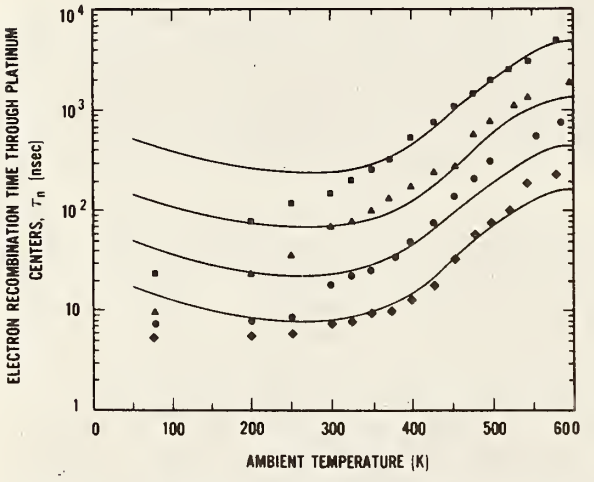

Figure 2. Electron recombination times through the platinum center in 2 Ω•cm p-type silicon as a function of temperature. The solid lines represent lifetimes calculated from eq (12), and the data points are measured lifetimes from ref. 13 for four n^+p diodes diffused with Pt. The diffusion temperatures are: ■, 850°C; ▲, 900°C; ●, 950°C; and ◆, 1000°C.

The situation in production-line device material is more difficult to assess than in specially prepared laboratory specimens, e.g., the case of Pt-doped silicon just discussed. The impurities are unknown *a priori*, and a DLTS scan is needed to help identify them. Often there are so many deep levels that the DLTS signals are hard to interpret due to overlapping peaks. An example of such a

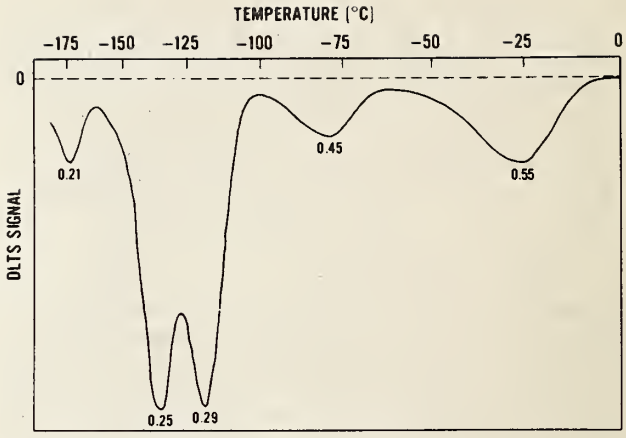

Figure 3. DLTS response of a high-voltage rectifier diode with experimental conditions optimized to resolve the large negative peak. The indicated energy for each level was obtained from an Arrhenius plot as a signature of each level for comparison purposes. The gate delay times were 89.5 ms and 191 ms. The reverse-bias sequence during the DLTS cycle was -17, -7, -17 V. The energies corresponding to these peaks are: 0.21, 0.25, 0.29, 0.45, and 0.55 eV in the order of increasing peak temperature.

complex, but resolved, case is shown in figure 3 for a commercial high-voltage rectifier diode.[14] There are five resolvable peaks which correspond to different impurities or impurity complexes. To date, only the highest temperature peak has been correlated with previous results and has been attributed to the gold acceptor state.

In this paper, we have shown a method for obtaining the parameters needed to model the recombination/generation lifetimes in silicon. The technique utilizes measurements of low-injection-level lifetimes as well as transient-capacitance results to obtain the needed parameters. This model can then be used to predict lifetime in devices under different injection conditions. We would also like to emphasize the need to measure lifetime and DLTS parameters in this way during the processing of devices as a means of monitoring deep levels. Some possible deleterious effects can be traced to the presence of underlying undesirable deep levels. Additional controlled experiments may be necessary to identify the sources of any deep-levels found by comparison with previously established signatures. Test structures (p-n junctions) can be included on the wafers to aid in the determination of those process steps that lead to degradation of device performance. Once such problems are diagnosed, processing can be modified to rid the device of the undesired recombination-altering deep-levels. If deep levels are intentionally added, the routine measurement of lifetime and DLTS will serve to monitor the deep-level addition process.

References

1. W. Shockley and W. T. Read, Phys. Rev. 87, 835 (1952); R. N. Hall, Phys. Rev. 87, 387 (1952).

2. S. K. Ghandhi, Semiconductor Power Devices (New York, Wiley & Sons, 1977), p. 5.

3. D. V. Lang, J. Appl. Phys. 45, 3023 (1974).

4. B. Lax and S. F. Neustadter, J. Appl. Phys. 25, 1148 (1954).

5. B. R. Gossick, J. Appl. Phys. 27, 905 (1956).

6. C. T. Sah, L. Forbes, L. L. Rosier, and A. F. Tasch, Jr., Solid-State Electron. 13, 759 (1970).

7. O. Engstrom and A. Alm, Solid-State Electron. 21, 1571 (1978).

8. S. D. Brotherton and J. Bicknell, J. Appl. Phys. 49, 667 (1978).

9. S. D. Brotherton and P. Bradley, J. Appl. Phys. 53, 1543 (1982).

10. R. H. Wu and A. R. Peaker, Solid-State Electron. 25, 643 (1982).

11. J. L. Moll, Physics of Semiconductors (New York, McGraw-Hill, Inc., 1964), p. 99.

12. S. D. Brotherton and J. E. Lowther, Phys. Rev. Lett. 44, 606 (1980).

13. M. D. Miller, H. Schade, and C. J. Neuse, J. Appl. Phys. 47, 2569 (1976).

14. W. R. Thurber, W. E. Phillips, and R. D. Larrabee, Measurement Techniques for High Power Semiconductor Materials and Devices: Annual Report Oct. 1, 1980 to Dec. 31, 1981, NBSIR 82-2552 (U.S. G.P.O., Washington, DC, 1982), p. 10.

Analysis of nonexponential transient capacitance in silicon diodes heavily doped with platinum

Willie E. Phillips and Jeremiah R. Lowney
Semiconductor Materials & Processes Division, National Bureau of Standards, Washington, D.C. 20234

(Received 4 October 1982; accepted for publication 4 January 1983)

An analysis having improved rigor has been made of the capacitance transient due to thermal emission from charged defect centers in a semiconductor depletion region. This analysis extends the range of applicability of capacitance–transient defect characterization techniques to nonexponential transient conditions which occur in diodes with trap densities of the same order as the net shallow dopant density or in diodes with somewhat smaller trap densities when defect centers are charged initially in only a part of the depletion region. An example of the improvement is shown for three silicon diodes heavily doped with platinum.

PACS numbers: 85.30.De, 71.55.Fr, 72.20.Jv, 85.30.Kk

INTRODUCTION

Defect characterization techniques such as deep-level transient spectroscopy (DLTS)[1] and isothermal transient capacitance (ITCAP)[2] utilize the ability of electrically active defect centers in depletion regions of semiconductors to trap and thermally to reemit charge carriers and thereby to affect the capacitance of the depletion region. It is assumed in conventional DLTS analysis that the measured capacitance transient varies exponentially with time. There are several causes of nonexponential behavior: the emission rate may depend on electric field, spatial nonuniformity of emission or capture rates may exist because of complexing, the density of the deep-level defects may not be small compared to the net shallow dopant density, the junction may not be abrupt, several trapping levels may exist (a sum of exponentials is nonexponential), and trap charging may occur in only part of the depletion region with moderate trap densities (a transient capacitance in series with a constant capacitance). It is the purpose of this paper to use a more rigorous analysis to investigate the capacitance transient in an abrupt-junction, platinum-doped silicon diode which exhibits no electric field or spatial dependencies, but may have: (1) densities of deep levels not small compared to that of shallow levels, or (2) trap charging over only a portion of the depletion layer with moderate trap densities (e.g., as occurs in profiling measurements). The work of Tomokage *et al.*[3] and that of Carcelle *et al.*[4] have considered (1), but not (2).

THEORY OF ANALYSIS

An analysis of a transient which does not exhibit an exponential behavior for either or both of the two reasons listed above can be made in transient capacitance measurements as follows. The transient behavior of the junction capacitance when the trap-filling bias is changed to a larger reverse bias, V_r, is controlled in n-type silicon by the electron emission rate from defect centers. The net time rate of change of n_t, the concentration per unit volume of electrons on the defect centers (i.e., traps) is given by[5]

$$\frac{dn_t}{dt} = e_p p_t - e_n n_t, \tag{1}$$

where e_n is the electron emission rate, e_p is the hole emission rate, and p_t is the concentration of holes on the defect centers. Because the trap must hold either an electron or a hole, the totality condition is satisfied:

$$n_t + p_t = N_t, \tag{2}$$

where N_t is the total defect center density. A differential equation in n_t can be obtained from Eqs. (1) and (2):

$$\frac{dn_t}{dt} + (e_n + e_p)n_t = e_p N_t. \tag{3}$$

The general solution of Eq. (3) is

$$n_t = C_1 \exp[\,-(e_n + e_p)t\,] + C_2. \tag{4}$$

The constants C_1 and C_2 can be evaluated at times zero and infinity. At $t = 0$, $n_t = C_1 + C_2 = n_{ti}$ and at $t = \infty$, $n_t = C_2 = n_{tf}$. Equation (4) can be written

$$n_t = n_{tf} + (n_{ti} - n_{tf})\exp[\,-(e_n + e_p)t\,]. \tag{5}$$

Under ideal one-sided step-junction conditions, the junction capacitance C at reverse bias V_r is[6]

$$C^{-2} = C_b^{-2} + \frac{2(V_r - V_c)}{q\epsilon A^2(N_d - n_t)}, \tag{6}$$

where C_b is the junction capacitance at some reduced trap-filling bias, V_c, A is the junction area, ϵ is the absolute dielectric constant (permittivity) of silicon, N_d is the shallow dopant density (assumed to be spatially uniform), and q is the electronic charge. (Note: SI units are used throughout this paper.) This equation is valid only if there is no significant compensation of the shallow dopants by the traps as discussed by Sah and Reddi.[7] The results of an extension of their theory for the present cases is given in the Appendix and a more general expression leading to a modification of Eq. (6) is obtained. The result of this analysis has shown that for sufficiently large reverse biases, there are ranges of bias voltages and times for which Eq. (6) is valid if the factor 2 is replaced by a dimensionless factor α which is constant during each menasurement but changes in value with experimental conditions.

This generalization of Eq. (6) can be solved for n_t to give

$$n_t = N_d - \frac{\alpha(V_r - V_c)C_b^2C^2}{q\epsilon A^2(C_b^2 - C^2)}. \quad (7)$$

At the initial time ($t = 0$), the reverse bias is reapplied (at the end of the trap-filling period), n_t is n_{ti}, and C is C_i. In the infinite time limit or final steady-state condition n_t is n_{tf} and C is C_f. Substitution of n_t, n_{ti}, and n_{tf} into Eq. (5) and solution for the exponential term gives:

$$\exp[-(e_n + e_p)t] = \frac{(C_b^2 - C_i^2)(C_f^2 - C^2)}{(C_b^2 - C^2)(C_f^2 - C_i^2)} \equiv C_r. \quad (8)$$

The right side of Eq. (8) is a capacitance ratio and will be called C_r. The same equation can also be expressed in terms of C as:

$$\frac{C^2}{C_b^2 - C^2} = \frac{C_f^2}{C_b^2 - C_f^2} + \left(\frac{C_i^2}{C_b^2 - C_i^2} - \frac{C_f^2}{C_b^2 - C_f^2}\right)e^{-t/\tau}, \quad (9)$$

where $\tau = 1/(e_n + e_p)$.

For the special case where the trap density is small compared to the shallow dopant density (i.e., $N_t/N_d \ll 1$), Eq. (9) reduces to the customary exponential form for sufficiently large C_b. Since C is bracketed by C_i and C_f, all the denominators in Eq. (9) will be approximately equal if $C_b^2 - C_f^2 \approx C_b^2 - C_i^2$. When $N_t/N_d \ll 1$ and C_b sufficiently large for exponentiality, $(C_f^2 - C_i^2)/C_f^2 = N_t/N_d$. Therefore, one obtains $C_b^2 - C_f^2 \approx C_b^2 - C_f^2(1 - N_t/N_d)$. This expression shows that in the limit of very low trap density ($N_t/N_d \to 0$), the denominators are nearly equal for all $C_b > C_f$. For more moderate trap densities, however, C_b must be sufficiently larger than C_f such that $(C_b^2 - C_f^2)/C_f^2 \gg N_t/N_d$. When the denominators in Eq. (9) are approximately equal,

$$C^2 - C_f^2 \simeq (C_i^2 - C_f^2)e^{-t/\tau}.$$

The difference of squares can be factored and for $C_i \approx C_f \approx C$, the sums $(C + C_f)$ and $(C_i + C_f)$ are approximately $2C_f$ so that

$$C \simeq C_f + (C_i - C_f)e^{-t/\tau}. \quad (10)$$

Therefore, the conventional analysis in which this exponential transient is assumed is valid for N_t/N_d small and for C_b sufficiently large. Under such conditions, a plot of log $[(C - C_f)/(C_i - C_f)] \equiv$ log C_n against time would be linear with a slope proportional to $1/\tau$. However, when these conditions are violated, as is shown below in the devices studied here, it is necessary to use the more rigorous analysis leading to Eq. (8) which predicts that a plot of log C_r against time would be linear with a slope proportional to $-1/\tau$ (equal to $-1/\tau$ if the natural logarithm is used).

DEVICE FABRICATION

The three devices used in this study are gated p^+n and n^+p diodes (device No. 10 of test pattern NBS-3)[8] and were fabricated on 3- to 5-Ω cm ⟨111⟩ n- or p-type silicon wafers. Boron predeposition and diffusion through 0.432-mm diameter openings in 500-nm of field oxide formed a 450-nm deep p^+n junction. The back side of this device was stripped and coated with a spun-on platinum emulsion followed by a drive-in at 850 °C for 2 h in a dry nitrogen ambient for device No. 1, and at 900 °C for 1 h for device No. 2. The residual platinum was etched from the back side. Contact opening, top metallization (aluminum), back metallization (gold plus 0.6% antimony), top metal definition, and a 10-min 500 °C microalloy in dry nitrogen completed the fabrication of the structure. The structure was hermetically packaged in a TO-100 header on a ceramic chip close to an electrically isolated temperature-sensing diode which was in good thermal contact with the test device because of high thermal conductivity of the ceramic. The n^+p diode (device No. 3) was fabricated in a complementary manner with boron replaced by phosphorus and with a platinum diffusion temperature of 1000 °C for 1 h.

DEVICE CHARACTERISTICS

The abruptness of the device junctions was tested; a plot of C^{-2} against V was found to be linear at room temperature and to obey the ideal diode equation, Eq. (6). The shallow dopant density N_d on the lightly doped side was calculated from these data. At the temperatures of the measurements (80–120 K), however, the C^{-2} versus V plots were nonideal as shown in Fig. 1. The theoretical curves (shown as solid lines) given by Eq. (A5) in the Appendix give a reasonable fit to the data (shown as circles) for devices No. 1 and 2. The

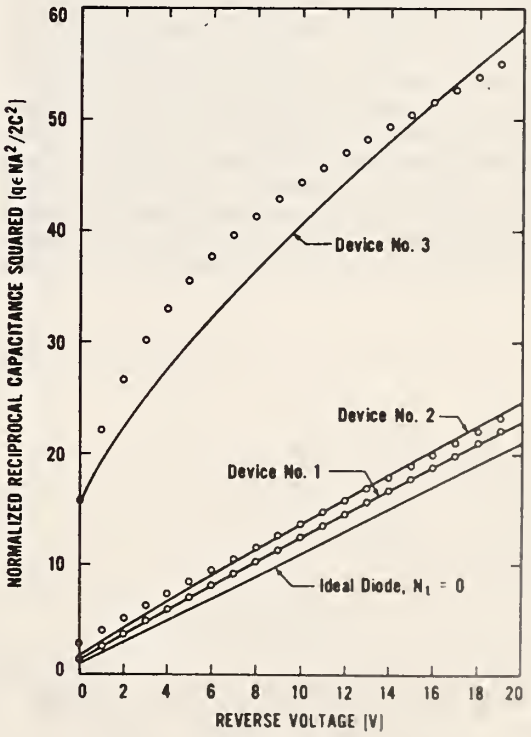

FIG. 1. Normalized C^{-2} vs V plots of experimental data on moderately heavily, and very heavily platinum-doped silicon diodes at low temperatures (devices No. 1–3, respectively). The solid lines are theoretical curves based on the present model, Eq. (A5), for these three devices and for an ideal diode.

trap and ionized dopant densities of Eq. (A5) N_T and N_d^+ were chosen to give a good fit both to these sets of data and to the transient capacitance data. The density ratios used for device No. 1 were $N_t/N_d = 0.19$ and $N_d^+/N_d = 0.78$ with a dopant density (donors) of $N_d = 1.08 \times 10^{15}$ cm^{-3}. The ratios for device No. 2 were $N_t/N_d = 0.38$ and $N_d^+/N_d = 0.77$ with $N_d = 1.21 \times 10^{15}$ cm^{-3}. In device No. 3, the dopant density (acceptors) was $N_a = 3.01 \times 10^{15}$ cm^{-3} and the density ratios were $N_t/N_a = 0.90$ and $N_a^-/N_a = 0.925$. The discrepancy between the model and the experimental data increases with increasing platinum density and is significant for device No. 3. It is not certain whether this discrepancy results from an inadequacy of the theory or from an inhomogeneity of trap density in the specimen near the junction.

The spatial dependence of the emission rate was investigated in device No. 2 by ITCAP measurements in incremental depletion layers of uniform width and electric field distributions. These test were accomplished by (1) applying a reverse bias of 2 V to the specimen diode, (2) waiting for equilibrium conditions, (3) partially collapsing the depletion region by reducing the bias to 0 V, (4) waiting a few seconds for the traps in the previously depleted region to fill with majority carriers, and (5) then restoring the depletion bias to 2 V. The capacitance transient response was recorded on an x–y recorder during and following these bias changes (see Fig. 2). The transient response was analyzed to obtain the emission rate. The measurements were repeated at a greater average distance from the junction by increasing the initial value of depletion bias to values greater than 2 V, but maintaining the same width of the active region (i.e., the portion of the space-charge region which upon reduction of the bias fills with majority carriers). Because the C^{-2} versus V plot was linear, an abrupt junction was assumed in which the total depletion depth varies as the square root of the voltage across the depletion layer. Thus the bias voltage during the trap-filling time V_c and the bias voltage during the time of observing the emission transient V_r can be selected so that the width of the active region is constant but is located at various distances from the junction. The voltage across this active portion of the depletion region was held constant as V_r and V_c (and thus the depth) were changed. The series of such measurements gave transients with a constant emission rate in the range of V_r of 2–20 V reverse bias. The tests were repeated with a larger average electric field (minimum $V_r = 5$ V) with the same resultant constant emission rate. A completely independent experiment with sulfur-doped silicon showed variations with both electric field and position of the active region. Therefore, for the case of this platinum-doped device, it was concluded that the emission rate is independent both of these electric field variations in the depletion region and of the position of the active region relative to the junction at distances greater than the zero-bias depletion depth.

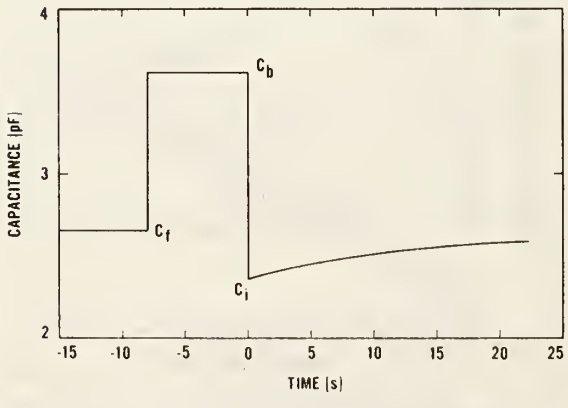

FIG. 2. Transient capacitance response against time of a p^+n silicon diode (device No. 2) heavily doped with platinum ($N_t/N_d \simeq 0.38$). Initial reverse bias is 20 V, charging reverse bias is 9.35 V, and the temperature is 87.7 K. $C_i = 2.36$ pF, $C_f = 2.65$ pF, and $C_b = 3.62$ pF.

RESULTS

A typical as-measured isothermal capacitance variation is shown in Fig. 2. The absence of a transient in C_b (the capacitance under trap-charging bias conditions) indicates that a slow-capture region resulting from spatially nonuniform capture rates[9,10] is not a problem for device No. 2. The same is true for device No. 1. A short transient is observed on device No. 3. When a transient is observed, one can wait until the traps in the slow-capture region are filled (as was done for device No. 3).

In Fig. 3, the transient response of Fig. 2 has been replotted (shown as circles) from digitized data as the conventional DLTS curve of log C_n against time. The plot is seen to be slightly nonlinear indicating that the measured capacitance transient is nonexponential. The instantaneous time constant (reciprocal of the emission rate) is proportional to the slope of the data and is dependent upon the time at which it is measured. The initial slope (shown as a dashed line) has a time constant of 12.7 sec. The nonexponentially of the capacitance transient is attributed to violation of the small N_t/N_d approximation (here $N_t/N_d = 0.38$) and to charging of traps in only part ($\sim 1/3$) of the depletion region. In contrast, a plot of the logarithm of C_r of Eq. (8) against time for the transient of Fig. 2 is shown as solid dots in Fig. 3. The solid line is a weighted linear regression fit to the data with a weighting factor of C_r and shows that these data are linear to within experimental error. The + 's are obtained from Eq. (A1) and are in good agreement with the experimental data. This agreement serves to justify the application of the present model to devices of this kind.

The capacitance ratios of a less heavily doped ($N_t/N_d = 0.19$) diode (device No. 1) are shown in Fig. 4. Again, the solid circles are log C_r, the open circles are log C_n, and the + 's are theoretical values of the same quantities as calculated by Eq. (A1). The linearity of the C_r values and the good agreement between the model presented in the Appendix and the experimental data are again obtained.

A more dramatic case is shown in Fig. 5 for the more heavily doped n^+p diode (device No. 3, $N_t/N_a = 0.90$) for two bias sequences. One curve shows data (circles) and the-

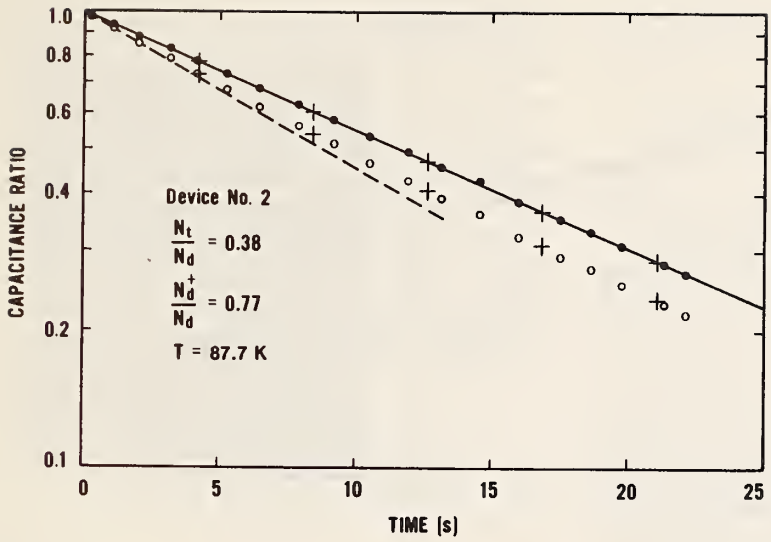

FIG. 3. Semilogarithmic digitized and normalized plot of the transient capacitance ratio C_n for the data of Fig. 2 (shown as open circles) against time. The dashed line is the initial slope. The solid circles represent the same data with the present more rigorous analysis which leads to the capacitance ratio C_r given by Eq. (8). The solid line is a weighted linear regression fit to the data of log C_r against time. The + 's are theoretical values calculated by use of Eq. (A1) with $C_i = 2.36$ pF, $C_f = 2.65$ pF, and $c_b = 3.62$ eV.

ory (×'s) for a trap-filling bias of 4 V, and the other shows data (squares) and theory (+ 's) for a trap-filling bias of 6 V. The bias during the emission transient for each is 9 V. The slight difference in the solid weighted linear regression lines through the C_r data is attributed to a systematic temperature difference of about 0.05 K between these runs. The solid circles and squares which correspond to log C_r at the beginning of the transient are below the fitted line as predicted by calculations from Eq. (A1). For this reason, experimental points before the time $\tau/2$ are excluded from the linear regression fit but are shown in Fig. 5. Even though the theory is less successful in predicting log C_n for this case, the agreement is very good for log C_r.

The significance of the linearity of the log C_r plots in Figs. 3, 4, and 5 is that the present analysis correctly accounts for the large trap density which leads to compensation of the partially deionized dopants, and for the unchanging capacitance in the part of the depletion region in which the traps are never charged. In Fig. 3, the time constant was found to be 16.88 ± 0.03 s, which is about 34% greater than the time constant indicated by the initial slope of the uncorrected capacitance data and about 16% greater than that of a straight line fitted to all of the uncorrected data. The above uncertainty value of ± 0.03 s is the one standard deviation uncertainty in the statistical fit only and does not include any instrumentation error. In Fig. 4, the time constant for the linear regression line is 13.92 ± 0.03 s which is 5% more than the uncorrected value obtained from a linear regression line fitted to the open circles. In Fig. 5, the time constant for the 9, 6, 9 V bias sequence (solid squares) is 70.20 ± 0.05 s,

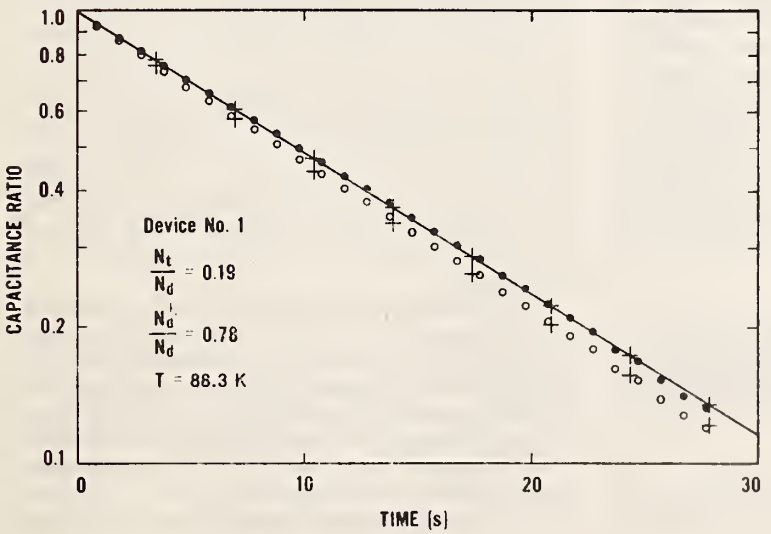

FIG. 4. Semilogarithmic digitized and normalized plot of the transient capacitance ratio C_n (shown as open circles) and C_r (shown as solid circles) against time for a p^+n silicon diode (device No. 1) moderately doped with platinum (N_t/N_d = 0.19). The solid line is a weighted linear regression fit to the data of log C_r against time. The + 's are theoretical values calculated by use of Eq. (A1) with $C_i = 4.55$ pF, $C_f = 4.72$ pF, and $C_b = 6.05$ pF as deduced by curve fitting. Experimental values for this capacitance transient are $C_i = 4.56$ pF, $C_f = 4.72$ pF, and $C_b = 6.03$ pF. Initial reverse bias is 5 V, charging bias is 2.5 V, and the temperature is 88.3 K.

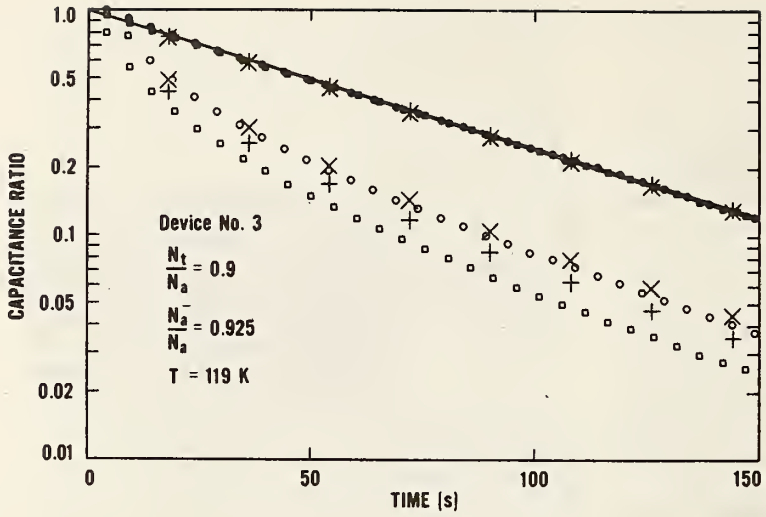

FIG. 5. Semilogarithmic digitized and normalized plot of the transient capacitance ratios C_n (shown as open circles and squares) and C_r (shown as solid circles and squares) against time for a n^+p silicon diode (device No. 3) very heavily doped with platinum ($N_t/N_a = 0.9$). Initial reverse bias is 9 V, charging reverse bias is 6 V for the squares and 4 V for the circles, and the temperature is 119 K. Measured capacitance for the squares are $C_i = 2.20$ pF, $C_f = 3.17$ pF, and $C_b = 3.39$ pF and for the circles are $C_i = 2.03$ pF, $C_f = 3.17$ pF, and $C_b = 3.62$ pF. The + 's are theoretical values for the 9, 6, 9 V biasing sequence ($C_i = 2.36$ pF, $C_f = 3.34$ pF, and $C_b = 3.65$ pF), and the ×'s are theoretical values for the 9, 4, 9 V biasing sequence ($C_i = 2.07$ pF, $C_f = 3.34$ pF, and $C_b = 3.94$ pF). The solid lines are linear regression fits to the two sets of data with points prior to $t = 35$ sec excluded.

which is about 4.5 times greater than the time constant indicated by the initial slope of the uncorrected capacitance data (open squares).

The time constants reported here for platinum in n-type silicon are in good agreement with an extrapolation of previous characterization measurements on devices similar to device No. 1.[11] Previous measurements on the p-type diodes[11] were made on heavily platinum-doped devices with biases in the nonlinear region of the C^{-2} versus V curve and give an extrapolated time constant less than the time constant reported here.

CONCLUSIONS

It is concluded that the use of the present more rigorous analysis can correct for the nonexponentiality introduced by a large density of defect centers which compensate the partially deionized shallow dopants at low temperature. It also corrects for trap charging in only a part of the depletion region at moderate levels of defect density. It was shown that the conventional exponential approximation is adequate only for small trap densities and that the correction for charging of these traps in only part of the depletion region decreases with decreasing trap density. The present analysis extends the range of applicability of transient capacitance techniques to conditions encountered in practical devices (e.g., N_t/N_d not $\ll 1$) and in more detailed measurements (e.g., deep level profiling).

ACKNOWLEDGMENT

This work was conducted as part of the Semiconductor Technology Program at NBS and was supported by the Division of Electric Energy Systems, Department of Energy (Task Order A021-EES).

APPENDIX

At low temperatures, the Fermi level lies close to the conduction band edge in n-type silicon or to the valence band edge in p-type silicon. If platinum is present, the Fermi level lies below the platinum donor level in p-type material or above the platinum acceptor level in n-type material. These levels then become charged and the platinum tends to compensate the shallow dopant. At sufficiently low temperatures significant compensation can occur in heavily Pt-doped diodes because the shallow dopants deionize. The result is that a p–n junction diode heavily doped with platinum has a C^{-2} versus V relationship which is nonlinear at low temperatures.

In order to model this situation, the theories of Sah and Reddi[7] and of Tomokage *et al.*[3] have been extended to include effects due to incomplete collapse of the space charge region and to compensation of the shallow dopant. Consider the space-charge region of a p^+n or an n^+p diode to be divided into three regions. The part of the space-charge region on the heavily doped side of the junction is neglected as in the previous work.[7,3] The effect of the platinum acceptor in p-type material or the platinum donor in n-type material is ignored as in the previous work[7,3] as well. For a p^+n diode the first region, nearest the metallurgical junction on the lightly doped n-type side, is taken to have a fixed bulk charge density of qN_d, where N_d is the shallow donor density. The extent of this region is determined by the crossing of the majority carrier quasi-Fermi level and the platinum donor level in p-type material or the platinum acceptor level in n-type material when the bias voltage is V_c, during the trap filling period.

The second region is taken to have a time-varying bulk charge density of $q(N_d - n_t)$ where n_t is the occupied trap density. The extent of this region is between the end of the first region and the crossing of the same quasi-Fermi level and platinum level when the bias voltage is V_r, the maximum reverse bias during which the transient emission is observed. The third region extends from the end of the second region and has a fixed bulk charge density of $q(N_d^+ - N_t)$ where N_d^+ is the average density of ionized donors and N_t is the

total trap density (i.e., all the traps are occupied and contribute to compensation). Since the quasi-Fermi level is close to the band edge in this region, there is some freezeout of the shallow dopant so that N_d^+ is less than N_d. The extent of this region is determined by the total width of the space charge region as found by integrating Poisson's equation twice. Since considerable compensation can occur between the filled traps and the ionized shallow dopants, this third region can be very wide. The result is a significant decrease in the junction capacitance, which is given by $\epsilon A/w(t)$ at high frequencies relative to trap emission rate, where $w(t)$ is the width of the space-charge region and A is the junction area.

The result of this extension of the Sah–Reddi model[7] is that the high frequency capacitance $C(t,V)$ is given by

$$C^{-1}(t,V_r) = \left(\frac{2}{q\epsilon A^2 N_d^+}\right)^{1/2} \frac{1}{(N_d - n_t)} \times \{\beta\gamma + [\beta^2\gamma^2 + N_d^+(N_d - n_t) \times (V_r + V_d - V_a - \beta\gamma^2/N_d^+)]^{1/2}\}, \quad \text{(A1)}$$

where

$$\beta = N_T - n_t + N_d - N_d^+ \quad \text{(A2)}$$

and

$$\gamma = \left[\frac{N_d^+ \phi}{N_d^+ - N_T}\right]^{1/2}. \quad \text{(A3)}$$

The built-in diffusion potential V_d is taken to be approximately 1 V, i.e., slightly less than the energy gap. The potential ϕ is the difference between the energy of the quasi-Fermi level and the trap level. This quantity is always greater than or equal to zero; if it were less than zero, the traps would be empty and their effect would disappear. The platinum donor level is approximately 320 meV[12] above the valence band, and the platinum acceptor level is approximately 230 meV below the conduction band.[12] The corresponding values for ϕ are approximately 250 meV in p-type material and 160 meV in n-type from estimates of the Fermi energy in material containing $\sim 10^{15}$ cm^{-3} shallow dopants at ~ 100 K.

The voltage V_a is given by

$$V_a = (q/2\epsilon)n_t\left[\epsilon A C^{-1}(\infty,V_c) - \left(\frac{2\epsilon\phi}{q(N_d^+ - N_T)}\right)^{1/2}\right]^2, \quad \text{(A4)}$$

where

$$C^{-1}(\infty,V) = \left(\frac{2}{q\epsilon A^2 N_d^+}\right)^{1/2} \{\rho\gamma + [\rho^2\gamma^2 + (N_d^+/N_d) \times (V + V_d - \rho\gamma^2 N_d/N_d^+)]^{1/2}\} \quad \text{(A5)}$$

and

$$\rho = (N_T + N_d - N_d^+)/N_d. \quad \text{(A6)}$$

In Eq. (A1) it is assumed that

$$n_t = N_T e^{-t/\tau}, \quad \text{(A7)}$$

which should be true at the low temperatures at which the measurements were made. Equations (A1)–(A7) are written for shallow donors and deep acceptor traps, but analogous equations exist for shallow acceptors and deep donor traps.

The values for the trap densities and ionized shallow dopant densities were obtained by fitting approximately both the C^{-2} versus V data and the total change in capacitance during the transient. The total shallow dopant density was obtained from room temperature C^{-2} versus V plots, which obeyed the ideal linear relationship for an abrupt junction. The amount of deionization found from these analyses was considered very reasonable when compared with calculations of the neutrality condition at these temperatures for samples containing no traps.

A comparison of Eq. (A1) and Eq. (6) shows that they are in agreement only if $\gamma = 0$, i.e., $\phi = 0$. However, if the reverse bias voltages V_c and V_r are sufficiently large and sufficiently close to each other, the effect of $\gamma > 0$ is to alter Eq. (6) such that for sufficiently long times, the form of Eq. (6) remains valid except that the factor 2 must be replaced by a dimensionless constant α which is in general greater than 2. This approximation is given by Eq. (7). The validity of this approximation is shown by the result of fitting the capacitance ratio C_r, given by Eq.(8), which is discussed in the *Results* section. The dependence of α on bias voltages and time is very complex, and it is better to use the fundamental Eq. (A1) to determine the validity of the approximation given by Eq. (7).

[1] D. V. Lang, J. Appl. Phys. **45**, 3023 (1974).

[2] W. E. Phillips and M. G. Buehler, in *Semiconductor Measurement Technology: Progress Report*, July 1 to September 30, 1976, edited by W. M. Bullis and J. F. Mayo-Wells, NBS Special Publication 400-36 (U.S. GPO, Washington, D.C., 1978), pp. 20–22.

[3] H. Tomokage, H. Nakashima, and K. Hashimoto, Jpn. J. Appl. Phys. **21**, 67 (1982).

[4] J. E. Carcelle, P. Cartujo, J. R. Morante, J. Barbolla, J. C. Brabant, and M. Brousseau, Rev. Phys. Appl. **15**, 843 (1980).

[5] M. G. Buehler, Solid-State Electron. **15**, 69 (1972).

[6] W. Shockley, Bell Sys. Tech. J. **28**, 435 (1949).

[7] C. T. Sah and V. G. K. Reddi, IEEE Trans. Electron Devices **ED-11**, 345 (1964).

[8] M. G. Buehler, *Semiconductor Measurement Technology: Microelectronic Test Pattern NBS-3 for Evaluating the Resistivity–Dopant Density Relationship of Silicon*, NBS Special Publication 400-22 (U.S. GPO, Washington, D.C., 1976).

[9] H. G. Grimmeiss, L. A. Ledebo, and E. Meijer, Appl. Phys. Lett. **36**, 307 (1980).

[10] J. A. Borsuk and R. M. Swanson, J. Appl. Phys. **52**, 6704 (1981).

[11] F. F. Oettinger and R. D. Larrabee, editors, *Measurement Techniques for High Power Semiconductor Materials and Devices: Annual Report, October 1, 1978 to September 30, 1979*, Interagency Report NBSIR 80-2061 (U.S. GPO., Washington, D.C., 1980), pp. 16-17.

[12] S. D. Brotherton, P. Bradley, and J. Bicknell, J. Appl. Phys. **50**, 3396 (1979).

APPENDIX C

Defects in Silicon, Proceedings Volume 83-9, W. M. Bullis and L. C. Kimerling, Eds., pp. 485-490 (Electrochemical Society, Pennington, N.J., 1983).

IMPROVED ANALYSIS PROCEDURES FOR DEEP-LEVEL MEASUREMENTS BY TRANSIENT CAPACITANCE*

W. E. Phillips, W. R. Thurber, and J. R. Lowney
National Bureau of Standards
Washington, DC 20234

The procedures reported here provide a way to analyze data from nonexponential transient capacitance measurements made under conditions such that (a) the trap density is not small compared with the net shallow dopant density or (b) the traps are charged in only a part of the depletion layer at moderate levels of trap density. This analysis requires C^{-2} vs V data to be linear over the voltage range used, which may be a small range at low temperatures because of the compensation effect of traps. The generalized analysis developed for isothermal transient capacitance (ITCAP) is extended to the more commonly used DLTS technique. The use of this analysis to obtain the correct emission rate from a nonexponential transient is illustrated by ITCAP and DLTS measurements for platinum in p^+n silicon diodes.

The growing popularity of transient-capacitance deep-level measurements (1) and the convenience of the deep-level transient spectroscopy (DLTS) method (2) have motivated this effort to extend the precision of our isothermal transient capacitance (ITCAP) method (3-4) to DLTS.

We have formulated a generalized approach to ITCAP (4), which we apply to DLTS. This approach is based upon a nearly linear C^{-2} vs V relationship for a p-n junction test diode. By making the depletion approximation, it is shown that the density of electrons on the defect centers, n_t, in the depletion region of a p^+n junction under reverse bias, V_r, is (4):

$$n_t = N_d - \frac{\alpha(V_r - V_c)C_b^2C^2}{q\varepsilon A^2(C_b^2 - C^2)}, \qquad (1)$$

where C is the junction capacitance, C_b is the capacitance at some reduced trap-filling bias, V_c, A is the junction area, ε is the absolute dielectric constant (permittivity) of silicon, N_d is the shallow-dopant density (assumed to be constant), q is the electronic charge, and α is a dimensionless parameter which is determined by the slope of the C^{-2} vs V relationship and which must remain sufficiently constant between V_r and V_c and throughout the capacitance transient.

*Contribution of the National Bureau of Standards. Not subject to copyright.

Figure 1 shows experimental C^{-2} *vs* V data for two platinum-doped p^+n silicon diodes of different platinum densities, along with theoretical curves calculated from the theories of Sah and Reddi (5) and Tomokage *et al.* (6) extended to include effects due to incomplete collapse of the space-charge region and to compensation of the shallow dopant by the platinum at low temperatures (4). We can see in Fig. 1 that the data are nearly linear over most of the voltage range, but with a slope that differs from the ideal case. The deviation between the data and the theory at low voltages for device no. 2 is not understood but may be due to inhomogeneity of the trap density near the junction.

Just after the bias voltage is changed from V_c to V_r, n_t is initially n_{ti} and C is initially C_i. After the resulting transient, n_t becomes finally n_{tf} and C becomes finally C_f. The time constant of the transient, τ, is related to a capacitance ratio given by:

$$C_r = \frac{(C_b^2 - C_i^2)(C_f^2 - C^2)}{(C_b^2 - C^2)(C_f^2 - C_i^2)} = e^{-t/\tau} . \qquad (2)$$

This relationship corrects for two conditions which are usually neglected in conventional DLTS measurements: 1) that the density of the deep-level defects may not be small compared to the net shallow dopant density, and 2) that trap charging may not take place throughout the depletion region at moderate levels of trap density. When the ratio of trap to net shallow dopant densities is not small, $N_t/N_d > 0.1$, both of these conditions will produce a nonexponential capacitance transient. A test for nonexponentiality has been reported (7) which requires a series of DLTS measurements for which $\tau = (t_1 - t_2)/\ln(t_1/t_2)$ is constant but the ratio of gate times t_1/t_2 varies over a wide range. A shift in the temperature location of the DLTS peak as t_1/t_2 varies indicates nonexponentiality. If nonexponentiality is found, the correct time constant can be calculated for the above two cases. This was demonstrated by use of the platinum-doped test diodes of Fig. 1.

The diodes of Fig. 1 were gated p^+n diodes fabricated on a 3 to 5 Ω·cm <111> n-type phosphorus-doped silicon wafer. Boron predeposition and diffusion through 0.432-mm diameter openings in 500 nm of field oxide formed a 450-nm deep p^+ region. The backside was stripped and coated with a spun-on platinum emulsion followed by a drive-in diffusion in a dry-nitrogen ambient at 850°C for 2 h for device no. 1 and at 900°C for 1 h for device no. 2. The residual platinum was etched from the backside with HF. Contact opening, top metallization (aluminum), back metallization (gold plus 0.6 percent antimony), top-metal definition, and a 10-min 500°C microalloy in dry nitrogen completed the fabrication of these test diodes.

A plot of log C_r vs time for ITCAP data for device no. 2 (N_t/N_d = 0.38) is shown in Fig. 2 as solid circles. The solid line is a weighted linear regression fit to these data. The open circles represent a conventional plot of the same data plotted as log $\left((C - C_f)/(C_i - C_f)\right)$. It is nonlinear (nonexponential). The dashed line shows the initial slope of the uncorrected transient which has a significantly shorter time constant than the remaining portions of the curve. The +'s are theoretical values for the corrected and uncorrected cases, calculated as done in Fig. 1 (4). This demonstrates that these corrections are significant.

Equation (2) can be rearranged as:

$$C(t,\tau) = \left[\frac{1}{C_b^2} + \frac{1}{\dfrac{C_b^2 C_f^2}{C_b^2 - C_f^2} + \left(\dfrac{C_b^2 C_i^2}{C_b^2 - C_i^2} - \dfrac{C_b^2 C_f^2}{C_b^2 - C_f^2}\right) e^{-t/\tau}}\right]^{-1/2} . \qquad (3)$$

The DLTS peak occurs when $d\left[C(t_1,\tau) - C(t_2,\tau)\right]/d\tau = 0$. The resultant equation can be solved iteratively for τ (8):

$$\tau = \frac{t_1 - t_2}{\ln\left(\dfrac{t_1}{t_2}\right) - \dfrac{1}{2}\ln\left(\dfrac{B(t_1)}{B(t_2)}\right)} , \qquad (4)$$

where

$$B(t) = 1 + A_1 e^{-t/\tau} + A_2 e^{-2t/\tau} + A_3 e^{-3t/\tau} + A_4 e^{-4t/\tau} ,$$

$$A_1 = F(C_b^2 + 3C_f^2)\, C_f^{-2} ,$$

$$A_2 = F^2(3C_b^2 + 3C_f^2)C_f^{-2} ,$$

$$A_3 = F^3(3C_b^2 + C_f^2)C_f^{-2} , \text{ and}$$

$$A_4 = F^4\, C_b^2 C_f^{-2} , \text{ where}$$

$$F = (C_i^2 - C_f^2)/(C_b^2 - C_i^2) .$$

Fortunately, the iteration converges very rapidly. The correction is most sensitive to an uncertainty in C_i and least sensitive to an uncertainty in C_b.

Figure 3 shows results of constant-voltage DLTS measurements performed using a double-boxcar system (9) on a diode from the same heavily platinum-doped silicon wafer used for the ITCAP measurements in Fig. 2. Normalized emission rate values, e/T^2, where $e = \tau^{-1}$, which have been corrected using eq (4), are shown in Fig. 3 as well as the uncorrected values obtained from the usual expression for emission rate which is valid only for exponential transients. Results are plotted for two different reverse bias sequences (i.e., V_r, V_c, V_r). It is evident from the figure that the correction

is much larger for the -10, -8, -10 V sequence. This is a consequence of charging only part of the depletion region during the -8 V trap-filling period. Although the uncorrected curves are significantly different, the corrected curves almost coincide as expected.

This correction of DLTS data requires the measurement of the same three capacitances as a function of temperature as for the ITCAP measurement. These capacitances, C_i, C_f, and C_b, were measured with a commercial capacitance bridge with a 15-mV, 1-MHz test signal. The use of 10 MHz for the DLTS measurement is not a problem because the traps are slow and the stray capacitances are negligible at these frequencies. The values for C_f and C_b were recorded on an x-y plotter in separate temperature runs. The determination of C_i is much more difficult as it is necessary to capture the leading edge of the transient. In order to measure the C_i associated with reasonably fast transients, modifications were made to the capacitance bridge to improve its response time. It was then possible, from oscilloscope photographs, to obtain $\Delta C = (C_f - C_i)$ for most of the temperature range normally covered by boxcar DLTS measurements, and only points in this range are included in Fig. 3. It was found that, within experimental error, ΔC was independent of temperature over the range measured. This is not unexpected as C_f is only slowly increasing with temperature in the same range. Thus in most applications the capacitance can be measured at three or four temperatures and then interpolated to obtain values at the specific temperatures required. Once these three capacitances are known, eq (4) can be solved.

As seen in Fig. 3 and from an examination of the equations, this more general DLTS analysis correction is largest for situations in which the deep level density is relatively large and the depletion region is incompletly collapsed, as is likely to be the case in depth-profiling experiments. It is also apparent that the analysis makes a large but similar correction in the emission rate of each point such that the slope is changed 2.5% or less. Cross sections as obtained from the extrapolated Arrhenius plots change about 30%. Mathematically, the analysis is correcting a constant-voltage DLTS experiment to make it equivalent to constant-capacitance DLTS where effects of deep-level density and incomplete charging are experimentally minimized. Thus constant-voltage DLTS measurements, which are simpler experimentally and can extend to faster time constants, can yield parameters which are at least as accurate as those obtained from constant-capacitance DLTS. The corrections reported here would not be required for constant-capacitance DLTS.

We wish to point out, however, that our correction technique is limited. It should not work as well if either the voltage difference $(V_r - V_c)$ is large compared to V_r or the gate times are far apart. The reason is that the slope α in eq (1) will vary significantly over an extended range of these parameters. To examine the effects of a different gate-time ratio on the correction, we mea-

sured the diode of Fig. 3 with the same bias voltage sequences but with a gate-time ratio of five instead of two. The results are shown in Fig. 4. In this figure note that the corrected data sets have a definite offset from each other in contrast to the coincident corrected sets in Fig. 3. Also, the corrected set in Fig. 4 with the -10, -8, -10 V bias sequence is the one which agrees best with the corrected sets in Fig. 3. This is reasonable, as the correction should work best for the data corresponding to the smaller voltage difference. These two figures illustrate the importance of keeping gate-time differences and voltage differences small and verifying the correction by repeating the measurement with a somewhat different gate-time ratio and voltage difference.

REFERENCES

1. C. T. Sah, L. Forbes, L. L. Rosier, and A. F. Tasch, Jr., Solid-St. Electron. 13, 759 (1970).
2. D. V. Lang, J. Appl. Phys. 45, 3023 (1974).
3. W. E. Phillips and M. G. Buehler, Semiconductor Measurement Technology: Progress Report, July 1 to September 30, 1976, edited by W. M. Bullis and J. F. Mayo-Wells, NBS Special Publ. No. 400-36 (U.S. G.P.O., Washington, DC, 1978), pp. 20-22.
4. W. E. Phillips and J. R. Lowney, Analysis of Nonexponential Transient Capacitance in Silicon Diodes Heavily Doped with Platinum, J. Appl. Phys. 54, 2786 (1983).
5. C. T. Sah and V. G. K. Reddi, IEEE Trans. Electron Devices ED-11, 345 (1964).
6. H. Tomokage, H. Nakashima, and K. Hashimoto, Jap. J. Appl. Phys. 21, 67 (1982).
7. W. R. Thurber, R. A. Forman, and W. E. Phillips, J. Appl. Phys. 53, 7397 (1982).
8. W. R. Thurber, W. E. Phillips, and R. D. Larrabee, Measurement Techniques for High Power Semiconductor Materials and Devices: Annual Report, October 1, 1980 to December 31, 1981, NBSIR 82-2552 (U.S. G.P.O., Washington, DC, 1982), pp. 49-52.
9. R. D. Larrabee, W. E. Phillips, and W. R. Thurber, Measurement Techniques for High Power Semiconductor Materials and Devices: Annual Report, October 1, 1979 to September 30, 1980, NBSIR 81-2325 (U.S. G.P.O., Washington, DC, 1981), pp. 8-9.

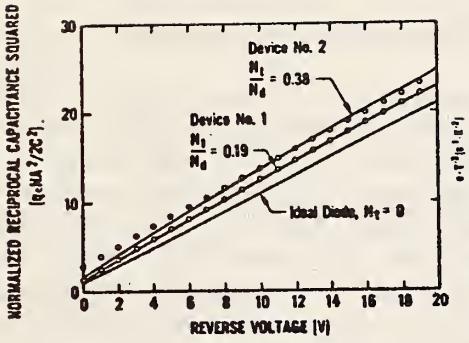

Fig.1. Normalized C^{-2}-V plots of experimental data on moderately and heavily platinum-doped silicon diodes at 88 K.

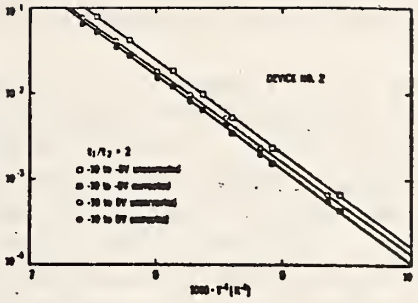

Fig. 3. An Arrhenius-type plot of scaled emission rate vs reciprocal temperature for a p^+n silicon diode heavily doped with platinum. Data were obtained using a DLTS system with an rf bridge operating at 10 MHz with a gate time ratio (t_2/t_1) of 2 for all points. Corrected values of emission rate were obtained from the general DLTS analysis discussed in the text for the two reverse bias sequences shown.

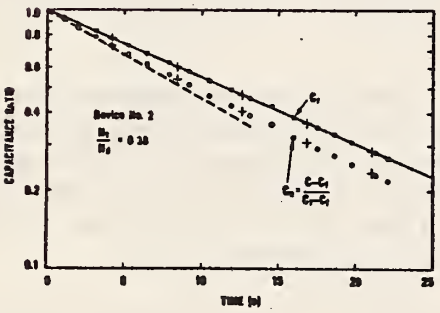

Fig. 2. Normalized semilogarithmic plot of the digitized transient capacitance response against time of a p^+n silicon diode (device no. 2) heavily doped with platinum at T = 88 K.

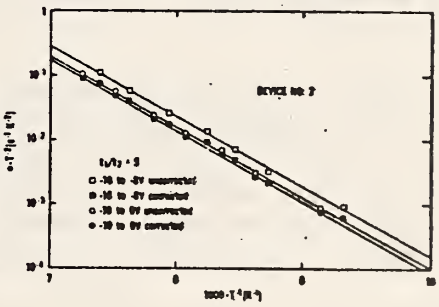

Fig. 4. An Arrhenius-type plot with all parameters the same as those for Fig. 3 except for the gate time ratio (t_2/t_1) which was five for all points.

APPENDIX D

Details and Listing of Lifetime-Predicting Computer Program

The program is divided into five separate routines: MAIN, ZEROIN, TEST, TAU, and TAUM. The MAIN routine inputs data, outputs results, and performs a few simple calculations. Subroutine ZEROIN calculates the Fermi energy by using a variant of the Newton-iteration scheme. It calls subroutine TEST to calculate the net ionized dopant and deep-level density for trial positions of the Fermi level. Subroutine TAU calculates lifetimes for single-level traps according to the equations in Ghandhi [1]. Subroutine TAUM calculates lifetimes for multilevel traps according to the equations in Moll [2].

The entry order of input data to the program is: three single-level donors, three single-level acceptors, first multilevel species (donor, then acceptor), second multilevel species (donor, then acceptor). There are five initial input parameters for each entry: 1) the name of the species (up to 8 characters); 2) the density of the species (cm^{-3}); 3) the appropriate energy level of the species in the energy gap (eV); 4) the degeneracy factor of the species appropriate to the level, which combines both electronic and lattice-related components; and 5) a flag, FLAG #1, which if false (F) means that donor energies are relative to the conduction band and acceptor energies are relative to the valence band, or if true (T) means that these energies are relative to the opposite bands. These parameters are entered for each species with a format (4A2, 1X, E9.4, 2F9.4, A1) with a blank line interpreted as a null entry.

Following these entries, one enters: the electron capture cross section (cm^2) and hole capture cross section (cm^2) for each species actually entered above (i.e., there are no blank lines). The format is (2E10.4). Following these entries, one enters: the starting temperature (K), the final temperature (K), and the incremental temperature (K) with a format (3F10.0). Finally one enters a second flag, FLAG #2, with format (L1).

This second flag is set to true (T) if it is desired that the lifetime be computed as a function of injection level. Otherwise, only the low-level recombination, high-level recombination, and space-charge generation lifetimes are computed. The program makes the assumption that the injected majority and minority carrier densities are equal, which is usually a good approximation if the trap densities are small compared to the dopant density so that a change in trap occupancy due to injection of carriers can be neglected. Therefore, this flag should be set to true only in material containing low trap density. For material which contains large trap densities, even if they are not effective recombination centers, a more involved analysis is needed to obtain lifetime as a function of injection ratio. These restrictions do not apply for the three lifetimes computed when the flag is false.

The numbers 1×10^{30} or 1×10^{-30} have been used in the program to avoid zero denominators. These largest and smallest numbers may be reflected in certain output quantities.

The format 4A2 is used to input and output literals. This format may have to be changed to suit other computers. The FORTRAN statement CHARACTER is used to define the literal variables and may not be available with some older versions of FORTRAN.

The outputs of this program are self-explanatory with the following remarks.

An error flag is printed when the ZEROIN search for the Fermi energy fails. Such an error would imply inconsistent input.

The zero of energy of E_F, the Fermi energy, is taken to be the top of the valence band. The zero of energy of all donor levels is the bottom of the conduction band and for all acceptor levels, the top of the valence band. For multilevel species, the donor level always precedes the acceptor level in the list.

The ionized density (ion. den.) refers to the presence of charge associated with the level. When shallow dopants are ionized, they are charged; when deep levels are ionized, they are also considered to be charged. An example of an input and output listing is given following the listing of the code.

```
C   MINORITY-CARRIER LIFETIME IN SILICON
C
C   PROGRAM CAN HANDLE UP TO 3 DONOR AND 3 ACCEPTOR SPECIES
C    (SINGLE LEVEL) ALONG WITH TWO MULTILEVEL SPECIES
C    OF THE SAME TYPE AS PLATINUM AND GOLD.
C
C
C   INPUT VARIABLE NAMES
C
C   LEVEL       NAME   DENSITY   ENERGY   DEGEN.  FL1
C
C   DONOR 1     NAME1  DN(1)     EN(1)    DG(1)   FL1(1)
C   DONOR 2     NAME2  DN(2)     EN(2)    DG(2)   FL1(2)
C   DONOR 3     NAME3  DN(3)     EN(3)    DG(3)   FL1(3)
C   ACCEPTOR 1  NAME4  DN(4)     EN(4)    DG(4)   FL1(4)
C   ACCEPTOR 2  NAME5  DN(5)     EN(5)    DG(5)   FL1(5)
C   ACCEPTOR 3  NAME6  DN(6)     EN(6)    DG(6)   FL1(6)
C   ML DONOR 1  NAME7  DN(7)     EN(7)    DG(7)   FL1(7)
C   ML ACCEP 1  NAME8  DN(8)     EN(8)    DG(8)   FL1(8)
C   ML DONOR 2  NAME9  DN(9)     EN(9)    DG(9)   FL1(9)
C   ML ACCEP 2  NAME10 DN(10)    EN(10)   DG(10)  FL1(10)
C
C   DONOR ENERGIES ARE REFERENCED TO CONDUCTION BAND
C   ACCEPTOR ENERGIES ARE REFERENCED TO VALENCE BAND
C   HOWEVER, THE REVERSE IS TRUE IF FL1 IS SET TRUE.
C
C
C
C                ELECTRON   HOLE
C   LEVEL        CAPTURE   CAPTURE
C                 CROSS-    CROSS-
C                SECTION   SECTION
C
C   DONOR 1       SE(1)     SH(1)
C   DONOR 2       SE(2)     SH(2)
C   DONOR 3       SE(3)     SH(3)
C   ACCEPTOR 1    SE(4)     SH(4)
C   ACCEPTOR 2    SE(5)     SH(5)
C   ACCEPTOR 3    SE(6)     SH(6)
C   ML DONOR 1    SE(7)     SH(7)
C   ML ACCEP 1    SE(8)     SH(8)
C   ML DONOR 2    SE(9)     SH(9)
C   ML ACCEP 2    SE(10)    SH(10)
C
C
C   A MODIFIED MKS SYSTEM OF UNITS IS USED
C      WITH CM REPLACING METERS
C
C   T = THE TEMPERATURE IN KELVIN
C   EG = THE ENERGY GAP OF SILICON IN ELECTRON VOLTS
```

```
C   EF = THE FERMI LEVEL IN EV ABOVE THE VALENCE BAND
C   CN = THE CONCENTRATION OF ELECTRONS IN THE CONDUCTION BAND IN CM-3
C   CP = THE CONCENTRATION OF HOLES IN THE VALENCE BAND IN CM-3
C   FNC = THE DENSITY OF STATES IN THE CONDUCTION BAND IN CM-3
C   FNV = THE DENSITY OF STATES IN THE VALENCE BAND IN CM-3
C   DI(1) - DI(10) = THE DENISTY OF IONIZED SPECIES
C      OF STATES NAME1 - NAME 10 IN CM-3
C   SE(1) - SE(10) = THE ELECTRON CAPTURE CROSS SECTIONS
C      OF STATES NAME1 - NAME10 IN CM+2
C   SH(1) - SH(2) = THE HOLE CAPTURE CRSS SECTIONS
C      OF STATES NAME1 - NAME6 IN CM+2
C   TAUNO(I) = HIGH LEVEL ELECTRON LIFETIME PARAMETER OF LEVEL I
C   TAUPO(I) = HIGH LEVEL HOLE LIFETIME PARAMETER OF LEVEL I
C
C   REFERENCES
C
C   1. GHANDHI, S. K., SEMICONDUCTOR POWER DEVICES:
C      PHYSICS OF OPERATION AND FABRICATION TECHNOLOGY,
C      PP. 2-31 (JOHN WILEY AND SONS, NEW YORK, 1977)
C
C   2. LARRABEE, R. D., THURBER, W. R., AND BULLIS, W. M.,
C      SEMICONDUCTOR MEASUREMENT TECHNOLOGY: A FORTRAN
C      PROGRAM FOR CALCULATING THE ELECTRICAL PROPERTIES
C      OF EXTRINSIC SILICON, NBS SPECIAL PUBLICATION 400-63,
C      OCTOBER, 1980
C
C   3. LARRABEE, R. D., PHILLIPS, W. E., AND THURBER, W. R.,
C      MEASUREMENT TECHNIQUES FOR HIGH POWER SEMICONDUCTOR
C      MATERIALS AND DEVICES: ANNUAL REPORT, OCTOBER 1, 1979
C      TO SEPTEMBER 30, 1980, PP. 33-37.
C
C   4. MOLL, J. L., PHYSICS OF SEMICONDUCTORS (NEW YORK,
C      MCGRAW-HILL,1964), P.92-101
C
C
C   MAIN PROGRAM HANDLES INPUT AND OUTPUT
C      AND CALLS THE FOLLOWING SUBROUTINES:
C         SUBROUTINE ZEROIN TO DETERMINE THERMAL EQUILIBRIUM CONDITIONS
C         SUBROUTINE TAU TO EVALUATE LIFETIME RELATED PARAMETERS
C
        EXTERNAL TEST
        DIMENSION NAME1(4),NAME2(4),NAME3(4)
        DIMENSION NAME4(4),NAME5(4),NAME6(4)
        DIMENSION NAME7(4),NAME8(4),NAME9(4),NAME10(4)
        DIMENSION DN(10),DI(10),EN(10),DG(10),ENT(10)
        DIMENSION SE(10),SH(10)
        DIMENSION TAUNO(10),TAUPO(10)
        COMMON NAME1,NAME2,NAME3,NAME4,NAME5,NAME6
        COMMON NAME7,NAME8,NAME9,NAME10
        CHARACTER*2 NAME1,NAME2,NAME3,NAME4,NAME5,NAME6
        CHARACTER*2 NAME7,NAME8,NAME9,NAME10
        CHARACTER*1 AFL1
        COMMON DN,DI,EN,DG
```

```
      COMMON T,CN,CP,EG,FNC,FNV,ALPHA,BETA
      COMMON TAUNO,TAUPO
      LOGICAL FL1,FL2
      DIMENSION FL1(10),AFL1(10)
C
C   INPUT THE CHARACTERISTICS OF THE ENERGY LEVELS
C
1     READ (4,50) NAME1,DN(1),EN(1),DG(1),AFL1(1)
50    FORMAT (4A2,1X,E9.4,2F9.4,A1)
      READ (4,50) NAME2,DN(2),EN(2),DG(2),AFL1(2)
      READ (4,50) NAME3,DN(3),EN(3),DG(3),AFL1(3)
      READ (4,50) NAME4,DN(4),EN(4),DG(4),AFL1(4)
      READ (4,50) NAME5,DN(5),EN(5),DG(5),AFL1(5)
      READ (4,50) NAME6,DN(6),EN(6),DG(6),AFL1(6)
      READ (4,50) NAME7,DN(7),EN(7),DG(7),AFL1(7)
      READ (4,50) NAME8,DN(8),EN(8),DG(8),AFL1(8)
      READ (4,50) NAME9,DN(9),EN(9),DG(9),AFL1(9)
      READ (4,50) NAME10,DN(10),EN(10),DG(10),AFL1(10)
C
C   IF DENSITY OF ANY STATE IS ZERO, RENAME IT TO '$$'
C     TO INDICATE THAT IT IS NOT PRESENT
C
      IF (DN(1).EQ.0.) NAME1(1)='$$'
      IF (DN(2).EQ.0.) NAME2(1)='$$'
      IF (DN(3).EQ.0.) NAME3(1)='$$'
      IF (DN(4).EQ.0.) NAME4(1)='$$'
      IF (DN(5).EQ.0.) NAME5(1)='$$'
      IF (DN(6).EQ.0.) NAME6(1)='$$'
      IF (DN(7).EQ.0.) NAME7(1)='$$'
      IF (DN(8).EQ.0.) NAME8(1)='$$'
      IF (DN(9).EQ.0.) NAME9(1)='$$'
      IF (DN(10).EQ.0.) NAME10(1)='$$'
C
    DO 100 I=1,10
    FL1(I)=.FALSE.
100 CONTINUE
      IF (NAME1(1).EQ.'$$') GO TO 210
    IF(AFL1(1).EQ.'T') FL1(1)=.TRUE.
      READ (4,200) SE(1),SH(1)
200   FORMAT (2E10.4)
210   IF (NAME2(1).EQ.'$$') GO TO 230
    IF(AFL1(2).EQ.'T') FL1(2)=.TRUE.
      READ (4,200) SE(2),SH(2)
230   IF (NAME3(1).EQ.'$$') GO TO 250
    IF(AFL1(3).EQ.'T') FL1(3)=.TRUE.
      READ (4,200) SE(3),SH(3)
250   IF (NAME4(1).EQ.'$$') GO TO 270
    IF(AFL1(4).EQ.'T') FL1(4)=.TRUE.
      READ (4,200) SE(4),SH(4)
270   IF (NAME5(1).EQ.'$$') GO TO 290
    IF(AFL1(5).EQ.'T') FL1(5)=.TRUE.
      READ (4,200) SE(5),SH(5)
290   IF (NAME6(1).EQ.'$$') GO TO 310
```

```
      IF(AFL1(6).EQ.'T') FL1(6)=.TRUE.
         READ (4,200) SE(6),SH(6)
310      IF (NAME7(1).EQ.'$$') GO TO 315
      IF(AFL1(7).EQ.'T') FL1(7)=.TRUE.
         READ (4,200) SE(7),SH(7)
315      IF (NAME8(1).EQ.'$$') GO TO 320
      IF(AFL1(8).EQ.'T') FL1(8)=.TRUE.
         READ (4,200) SE(8),SH(8)
320      IF (NAME9(1).EQ.'$$') GO TO 325
      IF(AFL1(9).EQ.'T') FL1(9)=.TRUE.
         READ (4,200) SE(9),SH(9)
325      IF (NAME10(1).EQ.'$$') GO TO 330
      IF(AFL1(10).EQ.'T') FL1(10)=.TRUE.
         READ (4,200) SE(10),SH(10)
C
C   ENTER TEMPERATURE RANGE OF INTEREST
C      START,END,STEP
C
330      READ (4,350) TSTART,TEND,TSTEP
350      FORMAT (3F10.0)
         IF (TSTEP.EQ.0.) TSTEP = 10.
         IF (TEND.EQ.0.) TEND=TSTART
         NT=INT(ABS((TEND-TSTART)/TSTEP))+1
         READ (4,352) FL2
352      FORMAT(L1)
         DO 1030 N=1,NT
         T=TSTART+(N-1)*TSTEP
C
C   PRELIMINARY COMPUTATIONS
C
C   EFME AND EFMH ARE THE EFFECTIVE MASSES OF ELECTRON AND HOLES
C      FROM BARBER, H. D., SOLID-STATE ELECTRONICS 10, 1039 (1967)
C      FITTED OVER THE TEMPERATURE RANGE FROM 0 TO 600 KELVIN
           EFME=(((((4.54649E-17*T-9.66067E-14)*T+8.04032E-11)*T-3.320130
     2  E-8)*T+6.83008E-6)*T-0.000161708)*T+1.0627
           EFMH=(((((1.11997E-16*T-2.596730E-13)*T+2.30049E-10)*T-9.67212
     2  E-8)*T+1.85678E-5)*T-0.000523548)*T+0.590525
C
C   FNC AND FNV ARE THE DENSITIES OF STATES IN THE BANDS
C   CONST=2*(2*PI*K*(FREE ELECTRON MASS)/H**2)**(3/2)
           CONST=4.829E15
           FNC=CONST*(EFME**1.5)*(T**1.5)
           FNV=CONST*(EFMH**1.5)*(T**1.5)
C
C   EG IS THE BANDGAP OF SILICON AT THE TEMPERATURE T
C      EG FROM FIT OF DATA OF MACFARLANE, PHYS. REV. 111, 1245 (1958)
           EG=(((-3.80977E-13*T+9.95E-10)*T-8.70110E-7)*T+0.0000323741)
     2  *T+1.15556
C
           CAYT=8.6173E-5*T
C
C   IF THE DEEP  LEVEL IS TIED TO THE  OPPOSITE BAND
C    FROM THE SHALLOW LEVELS (FL1(I)=TRUE), DO THE FOLLOWING
```

```
      DO 355 I=1,10
       IF(.NOT.FL1(I)) GO TO 355
       IF(N.EQ.1) ENT(I)=EN(I)
       EN(I)=EG-ENT(I)
355    CONTINUE
C
C
C   SET UP SEARCH FOR FERMI LEVEL
C
       EF=0.
       EFG=1.2
       RE=1.0E-6
       AE=1.0E-6
       IFLAG=0
       WRITE (7,360) T
360    FORMAT (1X,'FINDING FERMI LEVEL AT ',F5.0,' KELVIN')
       CALL ZEROIN (TEST,EF,EFG,RE,AE,IFLAG)
       WRITE (7,20)
20    FORMAT(1X)
       IF (IFLAG.GT.2) GO TO 1010
C
C   GUARD AGAINST ZERO DENOMINATORS
C
       IF (CN.EQ.0.) CN=1.E-30
       IF (CP.EQ.0.) CP=1.E-30
C
C   PRINT OUT PRESENT RESULTS
C
       WRITE (7,370)
370    FORMAT ('0',' NAME',5X,'DENSITY    ENERGY   DEGEN.   ',
     2  'CAPTURE CROSS SECTIONS')
       WRITE (7,380)
380    FORMAT (1X,39X,' ELECTRON     HOLE')
       WRITE (7,20)
       IF (NAME1(1).EQ.'$$') GO TO 390
       WRITE (7,450) NAME1,DN(1),EN(1),DG(1),SE(1),SH(1)
390    IF (NAME2(1).EQ.'$$') GO TO 400
       WRITE (7,450) NAME2,DN(2),EN(2),DG(2),SE(2),SH(2)
400    IF (NAME3(1).EQ.'$$') GO TO 410
       WRITE (7,450) NAME3,DN(3),EN(3),DG(3),SE(3),SH(3)
410    IF (NAME4(1).EQ.'$$') GO TO 420
       WRITE (7,450) NAME4,DN(4),EN(4),DG(4),SE(4),SH(4)
420    IF (NAME5(1).EQ.'$$') GO TO 430
       WRITE (7,450) NAME5,DN(5),EN(5),DG(5),SE(5),SH(5)
430    IF (NAME6(1).EQ.'$$') GO TO 432
       WRITE (7,450) NAME6,DN(6),EN(6),DG(6),SE(6),SH(6)
432    IF (NAME7(1).EQ.'$$') GO TO 435
       WRITE (7,450) NAME7,DN(7),EN(7),DG(7),SE(7),SH(7)
435    IF (NAME8(1).EQ.'$$') GO TO 437
       WRITE (7,450) NAME8,DN(8),EN(8),DG(8),SE(8),SH(8)
437    IF (NAME9(1).EQ.'$$') GO TO 440
       WRITE (7,450) NAME9,DN(9),EN(9),DG(9),SE(9),SH(9)
440    IF (NAME10(1).EQ.'$$') GO TO 460
```

```
      WRITE (7,450) NAME10,DN(10),EN(10),DG(10),SE(10),SH(10)
450   FORMAT (1X,4A2,2X,1PE10.3,0PF7.4,3X,0PF5.2,5X,2(1PE10.4,3X))
460   WRITE (7,470)
470   FORMAT ('0')
      WRITE (7,480)
480   FORMAT (1X,'THERMAL EQUILIBRIUM CONDITIONS')
      WRITE (7,20)
      WRITE (7,490)
490   FORMAT (1X,'  TEMP.    1000/T     EF',7X,'EG-EF',3X,
     2  ' CARRIER DENSITIES')
      WRITE (7,500)
500   FORMAT (1X,39X,' ELECTRON     HOLE')
      WRITE (7,20)
      RTEMP=1000./T
      EFV=EG-EF
      WRITE (7,510) T,RTEMP,EF,EFV,CN,CP
510   FORMAT (1X,F8.3,1X,F9.4,2X,F7.4,3X,F7.4,2X,2(1PE10.3,3X))
      WRITE (7,470)
C
C   COMPUTE TAUNO(I) AND TAUPO(I)
C
      DO 520 I=1,10
      TAUNO(I)=1.E30
520   TAUPO(I)=1.E30
C   CONST=(3*K/(FREE ELECTRON MASS))**0.5*(T/(EFFECTIVE MASS))**0.5
      CONST1=6.7421762E5*(T/EFME)**0.5
      CONST2=6.7421762E5*(T/EFMH)**0.5
      DO 540 I=1,10
      X=CONST1*SE(I)*DN(I)
      IF (X.EQ.0.) GO TO 530
      TAUNO(I)=1/X
530   X=CONST2*SH(I)*DN(I)
      IF (X.EQ.0.) GO TO 540
      TAUPO(I)=1/X
540   CONTINUE
C
C   CONTINUE PRINT-OUT OF THERMAL EQUILIBRIUM DATA
C
      WRITE (7,650)
650   FORMAT (1X,'  NAME     ION. DEN.  % IONIZED',
     2  '  TAUNO      TAUPO      TAUHIGH')
      WRITE (7,20)
C   HIGH LEVEL LIFETIME IS SUM OF TAUNO AND TAUPO FOR EACH STATE
C   NET HIGH LEVEL LIFETIME IS THE RECIPROCAL OF THE
C      SUM OF RECIPROCALS OF EACH STATE
      SUM=0
      IF (NAME1(1).EQ.'$$') GO TO 660
      X=TAUNO(1)+TAUPO(1)
      SUM=SUM+1/X
      Y=100*DI(1)/DN(1)
      WRITE (7,710) NAME1,DI(1),Y,TAUNO(1),TAUPO(1),X
660   IF (NAME2(1).EQ.'$$') GO TO 670
      X=TAUNO(2)+TAUPO(2)
```

```
          SUM=SUM+1/X
          Y=100*DI(2)/DN(2)
          WRITE (7,710) NAME2,DI(2),Y,TAUNO(2),TAUPO(2),X
670       IF (NAME3(1).EQ.'$$') GO TO 680
          X=TAUNO(3)+TAUPO(3)
          SUM=SUM+1/X
          Y=100*DI(3)/DN(3)
          WRITE (7,710) NAME3,DI(3),Y,TAUNO(3),TAUPO(3),X
680       IF (NAME4(1).EQ.'$$') GO TO 690
          X=TAUNO(4)+TAUPO(4)
          SUM=SUM+1/X
          Y=100*DI(4)/DN(4)
          WRITE (7,710) NAME4,DI(4),Y,TAUNO(4),TAUPO(4),X
690       IF (NAME5(1).EQ.'$$') GO TO 700
          X=TAUNO(5)+TAUPO(5)
          SUM=SUM+1/X
          Y=100*DI(5)/DN(5)
          WRITE (7,710) NAME5,DI(5),Y,TAUNO(5),TAUPO(5),X
700       IF (NAME6(1).EQ.'$$') GO TO 701
          X=TAUNO(6)+TAUPO(6)
          SUM=SUM+1/X
          Y=100*DI(6)/DN(6)
          WRITE (7,710) NAME6,DI(6),Y,TAUNO(6),TAUPO(6),X
701       IF (NAME7(1).EQ.'$$') GO TO 702
        HIN=TAUNO(7)*TAUNO(8)+TAUPO(7)*TAUNO(8)+TAUPO(7)*TAUPO(8)
        X=HIN/(TAUNO(8)+TAUPO(7))
          SUM=SUM+1/X
          Y=100*DI(7)/DN(7)
          WRITE (7,710) NAME7,DI(7),Y,TAUNO(7),TAUPO(7),X
          Y=100*DI(8)/DN(8)
          WRITE (7,710) NAME8,DI(8),Y,TAUNO(8),TAUPO(8),X
702       IF (NAME9(1).EQ.'$$') GO TO 720
        HIN=TAUNO(9)*TAUNO(10)+TAUPO(9)*TAUNO(10)+TAUPO(9)*TAUPO(10)
        X=HIN/(TAUNO(10)+TAUPO(9))
          SUM=SUM+1/X
          Y=100*DI(9)/DN(9)
          WRITE (7,710) NAME9,DI(9),Y,TAUNO(9),TAUPO(9),X
          Y=100*DI(10)/DN(10)
          WRITE (7,710) NAME10,DI(10),Y,TAUNO(10),TAUPO(10),X
710       FORMAT (1X,4A2,1X,5(1PE11.3))
720       WRITE (7,470)
          TAUHI=1/SUM
          WRITE (7,730) TAUHI
730       FORMAT (1X,'THE HIGH LEVEL TRAP RECOMBINATION LIFETIME ',
       2  'IS',1PE10.3,' SECONDS')
          WRITE (7,470)
C
C     EVALUATE LIFETIME UNDER DIFFERENT CONDITIONS
C        AND PRINT-OUT THE RESULTS
C     BUT  IF FL2 IS SET TO FALSE,
C     ONLY LOW INJECTION LEVEL LIFETIME IS EVALUATED
C     ALONG WITH THE SPACE-CHARGE GENERATION LIFETIME.
C     FOR FL2 TO BE SET TO TRUE THE TRAP DENSITIES
```

```
C   MUST BE SMALL COMPARED TO THE NET DOPANT DENSITY.
C
         CNE=CN
         CPE=CP
         R=CNE
         IF (CPE.GT.CNE) R=CPE
         R1=0.01*R
         R2=0.1*R
         SUM1=0.
         SUM2=0.
         SUM3=0.
         SUM4=0.
         SUM5=0.
         TAUMAX=1.E30
C
C   TAU1=LIMITING LIFETIME AT ZERO INJECTION LEVEL
C   TAU2=LIFETIME AT INJECTION LEVEL OF 0.01
C   TAU3=LIFETIME AT INJECTION LEVEL OF 0.10
C   TAU4=LIFETIME AT INJECTION LEVEL OF 1.00
C   TAU5=LIFETIME IN A DEPLETION LAYER
C
         TAU1=0.
      TAU2=0.
      TAU3=0.
      TAU4=0.
      TAU5=0.
         WRITE (7,740)
740      FORMAT (1X,'LIFETIME RELATED PARAMETERS')
         WRITE (7,20)
         WRITE (7,750)
750      FORMAT (1X,'  NAME     LOW LEVEL  I.R.=0.01  ',
     2  'I.R.=0.10  I.R.=1.00  DEPLETION LAYER')
         WRITE (7,20)
C
C
         DO 810 I=1,10
         IF (I.EQ.1.AND.NAME1(1).EQ.'$$') GO TO 810
         IF (I.EQ.2.AND.NAME2(1).EQ.'$$') GO TO 810
         IF (I.EQ.3.AND.NAME3(1).EQ.'$$') GO TO 810
         IF (I.EQ.4.AND.NAME4(1).EQ.'$$') GO TO 810
         IF (I.EQ.5.AND.NAME5(1).EQ.'$$') GO TO 810
         IF (I.EQ.6.AND.NAME6(1).EQ.'$$') GO TO 810
         IF (I.EQ.7.AND.NAME7(1).EQ.'$$') GO TO 810
         IF (I.EQ.8.AND.NAME8(1).EQ.'$$') GO TO 810
         IF (I.EQ.9.AND.NAME9(1).EQ.'$$') GO TO 810
         IF (I.EQ.10.AND.NAME10(1).EQ.'$$') GO TO 810
         IF (TAUNO(I).GE.TAUMAX) GO TO 810
         IF (TAUPO(I).GE.TAUMAX) GO TO 810
         IF(I.EQ.8.OR.I.EQ.10) GO TO 810
         IF(I.GE.7) GO TO 760
         CALL TAU(I,CNE,CPE,EN(I),0.,TAU1)
         SUM1=SUM1+1/TAU1
         IF(.NOT.FL2) GO TO 755
```

```
         CALL TAU(I,CNE,CPE,EN(I),R1,TAU2)
         SUM2=SUM2+1/TAU2
         CALL TAU(I,CNE,CPE,EN(I),R2,TAU3)
         SUM3=SUM3+1/TAU3
         CALL TAU(I,CNE,CPE,EN(I),R,TAU4)
         SUM4=SUM4+1/TAU4
755      CALL TAU(I,0.,0.,EN(I),0.,TAU5)
         SUM5=SUM5+1/TAU5
         GO TO 780
760    CALL TAUM(I,CNE,CPE,EN(I),EN(I+1),0.,TAU1)
         SUM1=SUM1+1/TAU1
         IF(.NOT.FL2) GO TO 770
       CALL TAUM(I,CNE,CPE,EN(I),EN(I+1),R1,TAU2)
         SUM2=SUM2+1/TAU2
       CALL TAUM(I,CNE,CPE,EN(I),EN(I+1),R2,TAU3)
         SUM3=SUM3+1/TAU3
       CALL TAUM(I,CNE,CPE,EN(I),EN(I+1),R,TAU4)
         SUM4=SUM4+1/TAU4
770    CALL TAUM(I,0.,0.,EN(I),EN(I+1),0.,TAU5)
         SUM5=SUM5+1/TAU5
780      IF (I.EQ.1) WRITE (7,800) NAME1,TAU1,TAU2,TAU3,TAU4,TAU5
         IF (I.EQ.2) WRITE (7,800) NAME2,TAU1,TAU2,TAU3,TAU4,TAU5
         IF (I.EQ.3) WRITE (7,800) NAME3,TAU1,TAU2,TAU3,TAU4,TAU5
         IF (I.EQ.4) WRITE (7,800) NAME4,TAU1,TAU2,TAU3,TAU4,TAU5
         IF (I.EQ.5) WRITE (7,800) NAME5,TAU1,TAU2,TAU3,TAU4,TAU5
         IF (I.EQ.6) WRITE (7,800) NAME6,TAU1,TAU2,TAU3,TAU4,TAU5
         IF (I.EQ.7) WRITE (7,800) NAME7,TAU1,TAU2,TAU3,TAU4,TAU5
         IF (I.EQ.9) WRITE (7,800) NAME9,TAU1,TAU2,TAU3,TAU4,TAU5
800      FORMAT (1X,4A2,1X,5(1PE11.3))
810      CONTINUE
C
820      WRITE (7,470)
         TAU1=1/SUM1
       IF(.NOT.FL2) GO TO 825
         TAU2=1/SUM2
         TAU3=1/SUM3
         TAU4=1/SUM4
825      TAU5=1/SUM5
         WRITE (7,830) TAU1
830      FORMAT (1X,'LOW LEVEL LIFETIME IS ',1PE10.3,
     2  ' SECONDS')
         WRITE (7,20)
         IF(.NOT.FL2) GO TO 865
         WRITE (7,840) TAU2
840      FORMAT (1X,'LIFETIME AT 0.01 I.R. IS ',1PE10.3,
     2  ' SECONDS')
         WRITE (7,20)
         WRITE (7,850) TAU3
850      FORMAT (1X,'LIFETIME AT 0.10 I.R. IS '1PE10.3,
     2  ' SECONDS')
         WRITE (7,20)
         WRITE (7,860) TAU4
860      FORMAT (1X,'LIFETIME AT 1.00 I.R. IS ',1PE10.3,
```

```
     2  ' SECONDS')
865       WRITE (7,20)
          WRITE (7,870) TAU5
870       FORMAT (1X,'LIFETIME IN A DEPLETION LAYER IS ',
     2  1PE10.3,' SECONDS')
          WRITE (7,880)
880       FORMAT ('1')
          GO TO 1030
1010      WRITE (7,1020) IFLAG
1020      FORMAT (1X,'ERROR FLAG = ',I2)
1030   CONTINUE
          END
C    SUBROUTINE ZEROIN(F,B,C,RE,AE,IFLAG)
C
C    SANDIA MATHEMATICAL PROGRAM LIBRARY
C    MATHEMATICAL COMPUTING SERVICES DIVISION 5422
C    SANDIA LABORATORIES
C    P.O. BOX 5800
C    ALBUQUERQUE, NEW MEXICO 87115
C
C    CONTROL DATA 6600 VERSION 4.5, 1 NOVEMBER 1971
C
C    MODIFIED BY D. KAHANER, NBS DIVISION 713.
C
C    ABSTRACT:
C       ZEROIN SEARCHES FOR A ZERO OF A FUNCTION F(X) BETWEEN
C       THE GIVEN VALUES B AND C UNTIL THE WIDTH OF INTERVAL
C       (B,C) HAS COLLAPSED TO WITHIN A TOLERANCE SPECIFIED BY
C       THE STOPPING CRITERION, ABS(B-C).LE.2.*(RW*ABS(B)+AE).
C
C    DESCRIPTION OF ARGUMENTS:
C       F     - NAME OF THE REAL VALUED EXTERNAL FUNCTION.
C               THIS NAME MUST BE IN AN EXTERNAL STATEMENT
C               IN THE CALLING PROGRAM.
C               F MUST BE A FUNCTION OF ONE REAL ARGUMENT.
C       B     - ONE END OF THE INTERVAL (B,C).
C               THE VALUE RETURNED FOR B USUALLY IS THE
C               BETTER APPROXIMATION OF F.
C       C     - THE OTHER END OF THE INTERVAL (B.C).
C       RE    - THE RELATIVE ERROR USED FOR RW
C               IN THE STOPPING CRITERION.
C               IF THE REQUESTED RE IS LESS THAN THE MACHINE
C               PRECISION, THEN RW IS SET TO APPROXIMATELY
C               THE MACHINE PRECISION.
C       AE    - THE ABSOLUTE ERROR USED IN THE STOPPING
C               CRITERION.  IF THE GIVEN INTERVAL (B,C)
C               CONTAINS THE ORIGIN, THEN A NONZERO VALUE
C               SHOULD BE CHOSEN FOR AE.
C       IFLAG - RETURNS A STATUS OF THE RESULTS INDICATING
C               WHICH OF THE FOLLOWING CONDITIONS HOLD:
C
C                     A - ABS(B-C).LE.2.*(RW*ABS(B)+AE).
C                     B - F(B)*F(C).LT.0.
```

```
C                   C - ABS(F(B)).LE.ABS(F(C)).
C                   D - ABS(F(B"OUT")).LE.
C                       MAX(ABS(F(B"IN")),ABS(F(C"IN"))).
C                   E - NUMBER OF EVALUATIONS OF F(X),LE.500.
C
C                IFLAG=1 INDICATES NORMAL CASE
C                        ALL CONDITIONS ABOVE HOLD.
C                IFLAG=2 INDICATES F(B)=0.
C                        CONDITION A MAY NOT HOLD.
C                IFLAG=3 INDICATES CONDITIONS A, B, C, AND E
C                        HOLD, BUT CONDITION D DOES NOT.
C                        THE INTERVAL (B,C) PROBABLY CONTAINS
C                        A SINGLULAR POINT OF THE FUNCTION F.
C                IFLAG=4 INDICATES CONDITIONS A AND E HOLD,
C                        BUT CONDITION B DOES NOT.
C                        A LOCAL MINIMUM OF F(X) IN (B,C)
C                        MAY HAVE BEEN FOUND.
C                IFLAG=5 INDICATES SEARCH WAS ABORTED
C                        WHEN CONDITION E FAILED.
C
C   REFERENCES:
C      1.   L. F. SHAMPINE AND H. A. WATTS, ZEROIN,
C           A ROOT-SOLVING CODE, SC-TM-70-631, SEPT., 1970.
C      2.   T. J. DEKKER, FINDING A ZERO BY MEANS
C           OF SUCCESSIVE LINEAR INTERPOLATION,
C           *CONSTRUCTIVE ASPECTS OF THE FUNDAMENTAL THEORM
C           OF ALGEBRA*, EDITED BY D. DEJON AND P. HENRICI,
C            1969.
C      3.   L. F. SHAMPINE AND R. C. ALLEN, NUMERICAL
C           COMPUTING -- AN INTRODUCTION.
C
C   SEE NBS SPECIAL PUBLICATION 400-63, PP. 28-30
C
        SUBROUTINE ZEROIN(F,B,C,RE,AE,IFLAG)
        DATA ER/6.0E-8/
C   INITIALIZE IN PORTABLE MANNER
C   DATA ER/0.0/
C   IF (ER.EQ.0.) ER=4.*(R1MACH(4))
C
        RW=AMAX1(RE,ER)
        IC=0
        ACBS=ABS(B-C)
        A=C
        FA=F(A)
        FB=F(B)
        FC=FA
        KOUNT=2
        FX=AMAX1(ABS(FB),ABS(FC))
C
1       IF (ABS(FC).GE.ABS(FB)) GO TO 2
C   PERFORM INTERCHANGE
        A=B
        FA=FB
```

```
      B=C
      FB=FC
      C=A
      FC=FA
C
2     CMB=0.5*(C-B)
      ACMB=ABS(CMB)
      TOL=RW*ABS(B)+AE
C
C   TEST STOPPING CRITERION
      IF(ACMB.LE.TOL) GO TO 10
C
C   CALCULATE NEW ITERATE IMPLICITLY AS B+P/Q
C   WHERE  P.GE.0. HAS BEEN GUARANTEED.
C   THE IMPLICIT FORM IS USED TO PREVENT OVERFLOW.
      P=(B-A)*FB
      Q=FA-FB
      IF (P.GE.0.) GO TO 3
      P=-P
      Q=-Q
C
C   UPDATE A AND CHECK FOR SATISFACTORY REDUCTION
C      IN THE SIZE OF OUR BOUNDING INTERVAL.
3       A=B
        FA=FB
        IC=IC+1
        IF (IC.LT.4) GO TO 4
        IF (8.*ACMB.GE.ACBS) GO TO 6
        IC=0
        ACBS=ACMB
C
C   TEST FOR TOO SMALL A CHANGE
4       IF (P.GT.ABS(Q)*TOL) GO TO 5
C
C   INCREMENT BY TOLERANCE
        B=B+SIGN(TOL,CMB)
        GO TO 7
C
C   ROOT OUGHT TO BE BETWEEN B AND (C+B)/2.
5       IF (P.GE.CMB*Q) GO TO 6
C
C   INTERPOLATE
        B=B+P/Q
        GO TO 7
C
C   BISECT THE INTERVAL
6       B=0.5*(C+B)
C
C   COMPUTATION FOR NEW ITERATE B HAS BEEN COMPLETED.
7       FB=F(B)
        IF (FB.EQ.0.) GO TO 11
        KOUNT=KOUNT+1
        IF (KOUNT.GT.500) GO TO 15
```

```
C
C    DECIDE IF NEXT STEP IS INTERPOLATION OR EXTRAPOLATION
          IF (SIGN(1.0,FB).NE.SIGN(1.0,FC)) GO TO 1
          C=A
          FC=FA
          GO TO 1
C
C
C    FINISHED.  PROCESS RESULTS FOR PROPER SETTING OF IFLAG.
C
10        IF (FB*FC.GT.0.) GO TO 13
          IF (ABS(FB).GT.FX) GO TO 12
          IFLAG=1
          RETURN
11        IFLAG=2
          RETURN
12        IFLAG=3
          RETURN
13        IFLAG=4
          RETURN
15        IFLAG=5
          RETURN
          END
C    FUNCTION TEST(EF)
C    THIS EXTERNAL FUNCTION DEFINES THE PARAMETER 'TEST'.
C    SUBROUTINE ZEROIN LOCATES THE VALUE WHICH MINIMIZES 'TEST'.
C
          FUNCTION TEST(EF)
          DIMENSION NAME1(4),NAME2(4),NAME3(4)
          DIMENSION NAME4(4),NAME5(4),NAME6(4)
          DIMENSION NAME7(4),NAME8(4),NAME9(4),NAME10(4)
          DIMENSION DN(10),DI(10),EN(10),DG(10)
          DIMENSION TAUNO(10),TAUPO(10)
          COMMON NAME1,NAME2,NAME3,NAME4,NAME5,NAME6
          COMMON NAME7,NAME8,NAME9,NAME10
          CHARACTER*2 NAME1,NAME2,NAME3,NAME4,NAME5,NAME6
          CHARACTER*2 NAME7,NAME8,NAME9,NAME10
          COMMON DN,DI,EN,DG
          COMMON T,CN,CP,EG,FNC,FNV,ALPHA,BETA
          COMMON TAUNO,TAUPO
C    LEVELS NOT PRESENT HAVE FIRST TWO CHAR. OF NAME = '$$'
C
          CAYT=8.6173E-5*T
C
C    COMPUTATION OF CN
          CN=0.
          ALPHA=(EF-EG)/CAYT
          IF (ALPHA.GT.1.) GO TO 10
          IF (ALPHA.LE.-80.) GO TO 20
C    THE FOLLOWING EQUATION IS USED FOR ALPHA BETWEEN -80 AND +1
          CN=FNC/((EXP(-ALPHA))+0.27)
          GO TO 20
C    THE FOLLOWING EQUATION IS USED FOR ALPHA GREATER THAN +1
```

```
10        CN=FNC*0.752253*((ALPHA*ALPHA+1.7)**0.75)
C
C    COMPUTATION OF CP
20        CP=0.
          BETA=-EF/CAYT
          IF (BETA.GT.1.) GO TO 30
          IF (BETA.LE.-80.) GO TO 40
C    THE FOLLOWING EQUATION IS USED FOR BETA BETWEEN -80 AND +1
          CP=FNV/((EXP(-BETA))+0.27)
          GO TO 40
C    THE FOLLOWING EQUATION IS USED FOR BETA GREATER THAN +1
30        CP=FNV*0.752253*((BETA*BETA+1.7)**0.75)
C
C    COMPUTATION OF DI(1)
40        DI(1)=0.
          IF (NAME1(1).EQ.'$$') GO TO 60
          POWER=(EF-EG+EN(1))/CAYT
          IF (POWER.GE. 80.) GO TO 60
          IF (POWER.LE.-80.) GO TO 50
          DI(1)=DN(1)/(1.+(EXP(POWER)*DG(1)))
          GO TO 60
50        DI(1)=DN(1)
C
C    COMPUTATION OF DI(2)
60        DI(2)=0.
          IF (NAME2(1).EQ.'$$') GO TO 80
          POWER=(EF-EG+EN(2))/CAYT
          IF (POWER.GE.80.) GO TO 80
          IF (POWER.LE.-80.) GO TO 70
          DI(2)=DN(2)/(1.+(EXP(POWER)*DG(2)))
          GO TO 80
70        DI(2)=DN(2)
C
C    COMPUTATION OF DI(3)
80        DI(3)=0.
          IF (NAME3(1).EQ.'$$') GO TO 100
          POWER=(EF-EG+EN(3))/CAYT
          IF (POWER.GE.80.) GO TO 100
          IF (POWER.LE.-80.) GO TO 90
          DI(3)=DN(3)/(1.+(EXP(POWER)*DG(3)))
          GO TO 100
90        DI(3)=DN(3)
C
C    COMPUTATION OF DI(7)
100       DI(7)=0.
          T1=0.
          T2=0.
          IF (NAME7(1).EQ.'$$') GO TO 120
          POWER1=(EF-EG+EN(7))/CAYT
          POWER2=(EF-EN(8))/CAYT
          IF(POWER1.GE.80.) GO TO 120
          IF(POWER1.LE.-80.) GO TO 105
          T1=EXP(POWER1)*DG(7)
```

```
105       IF((POWER1+POWER2).GE.80) GO TO 120
          IF((POWER1+POWER2).LE.-80) GO TO 110
          T2=EXP(POWER1+POWER2)/DG(8)*DG(7)
110       DI(7)=DN(7)/(1+T1+T2)
C
C
C    COMPUTATION OF DI(9)
120       DI(9)=0.
          T1=0.
          T2=0.
          IF (NAME9(1).EQ.'$$') GO TO 200
          POWER1=(EF-EG+EN(9))/CAYT
          POWER2=(EF-EN(10))/CAYT
          IF(POWER1.GE.80.) GO TO 200
          IF(POWER1.LE.-80.) GO TO 125
          T1=EXP(POWER1)*DG(9)
125       IF((POWER1+POWER2).GE.80) GO TO 200
          IF((POWER1+POWER2).LE.-80) GO TO 130
          T2=EXP(POWER1+POWER2)/DG(10)*DG(9)
130       DI(9)=DN(9)/(1+T1+T2)
C
C    COMPUTATION OF DI(4)
200       DI(4)=0.
          IF (NAME4(1).EQ.'$$') GO TO 220
          POWER=(EN(4)-EF)/CAYT
          IF (POWER.GT.80.) GO TO 220
          IF (POWER.LE.-80.) GO TO 210
          DI(4)=DN(4)/(1.+(EXP(POWER)*DG(4)))
          GO TO 220
210       DI(4)=DN(4)
C
C    COMPUTATION OF DI(5)
220       DI(5)=0.
          IF (NAME5(1).EQ.'$$') GO TO 240
          POWER=(EN(5)-EF)/CAYT
          IF (POWER.GE.80.) GO TO 240
          IF (POWER.LE.-80.) GO TO 230
          DI(5)=DN(5)/(1.+(EXP(POWER)*DG(5)))
          GO TO 240
230       DI(5)=DN(5)
C
C    COMPUTATION OF DI(6)
240       DI(6)=0.
          IF (NAME6(1).EQ.'$$') GO TO 260
          POWER=(EN(6)-EF)/CAYT
          IF (POWER.GT.80.) GO TO 260
          IF (POWER.LE.-80.) GO TO 250
          DI(6)=DN(6)/(1.+(EXP(POWER)*DG(6)))
          GO TO 260
250       DI(6)=DN(6)
C
C    COMPUTATION OF DI(8)
260       DI(8)=0.
```

```
      T1=0.
      T2=0.
      IF (NAME8(1).EQ.'$$') GO TO 280
      POWER1=(EN(8)-EF)/CAYT
      POWER2=(-EN(7)-EF+EG)/CAYT
      IF(POWER1.GE.80.) GO TO 280
      IF(POWER1.LE.-80.) GO TO 265
      T1=EXP(POWER1)*DG(8)
265   IF((POWER1+POWER2).GE.80) GO TO 280
      IF((POWER1+POWER2).LE.-80) GO TO 270
      T2=EXP(POWER1+POWER2)/DG(7)*DG(8)
270   DI(8)=DN(8)/(1+T1+T2)
C   COMPUTATION OF DI(10)
280   DI(10)=0.
      T1=0.
      T2=0.
      IF (NAME10(1).EQ.'$$') GO TO 300
      POWER1=(EN(10)-EF)/CAYT
      POWER2=(-EN(9)-EF+EG)/CAYT
      IF(POWER1.GE.80.) GO TO 300
      IF(POWER1.LE.-80.) GO TO 285
      T1=EXP(POWER1)*DG(10)
285   IF((POWER1+POWER2).GE.80) GO TO 300
      IF((POWER1+POWER2).LE.-80) GO TO 290
      T2=EXP(POWER1+POWER2)/DG(9)*DG(10)
290   DI(10)=DN(10)/(1+T1+T2)
C
C   TESTING TO SEE HOW CLOSE TO
C   THE PARAMETER TEST IS THE NET DENSITY OF RESIDUAL CHARGES
C      WHEN THE FERMI LEVEL IS AT ITS PRESENT LOCATION
300     TEST=(CN+DI(4)+DI(5)+DI(6))-(CP+DI(1)+DI(2)+DI(3))
        TEST=TEST+DI(8)+DI(10)-DI(7)-DI(9)
        RETURN
        END
        SUBROUTINE TAU(I,CNE,CPE,ENF,EDN,TAUX)
C
C   SUBROUTINE TO COMPUTE SPACE-CHARGE NEUTRAL LIFETIMES
C   FOR SINGLE LEVEL TRAPS
C
C   DESCRIPTION OF ARGUMENTS:
C      I     - INDEX RANGING FROM 1 TO 6 SPECIFYING THE ENERGY LEVEL
C      CNE   - THERMAL EQUILIBRIUM DENSITY OF ELECTRONS
C      CPE   - THERMAL EQUILIBRIUM DENSITY OF HOLES
C      ENF   - POSITION OF THE TRAP LEVEL
C       EDN  - DENSITY OF EXCESS ELECTRON-HOLE PAIRS
C      TAUX  - COMPUTED VALUE OF THE LIFETIME
C
        DIMENSION NAME1(4),NAME2(4),NAME3(4)
        DIMENSION NAME4(4),NAME5(4),NAME6(4)
        DIMENSION NAME7(4),NAME8(4),NAME9(4),NAME10(4)
        DIMENSION DN(10),DI(10),EN(10),DG(10)
        DIMENSION SE(10),SH(10)
        DIMENSION TAUN0(10),TAUP0(10)
```

```
      COMMON NAME1,NAME2,NAME3,NAME4,NAME5,NAME6
      COMMON NAME7,NAME8,NAME9,NAME10
      CHARACTER*2 NAME1,NAME2,NAME3,NAME4,NAME5,NAME6
      CHARACTER*2 NAME7,NAME8,NAME9,NAME10
      COMMON DN,DI,EN,DG
      COMMON T,CN,CP,EG,FNC,FNV,ALPHA,BETA
      COMMON TAUNO,TAUPO
C
C   COMPUTE GHANDHI'S FACTORS N1 AND P1 CORRECTED FOR DEGENERACY
C
      CAYT=8.6173E-5*T
      IF (I.GT.3) GO TO 10
      ZN1=FNC*EXP(-(ENF)/CAYT)/DG(I)
      ZP1=FNV*EXP(-(EG-ENF)/CAYT)*DG(I)
      GO TO 20
10    ZN1=FNC*EXP(-(EG-ENF)/CAYT)*DG(I)
      ZP1=FNV*EXP(-ENF/CAYT)/DG(I)
C
C   EVALUATE LIFETIME EXPRESSION
C
20    DENOM=CNE+CPE+EDN
      IF (DENOM.EQ.0.) GO TO 30
      X=TAUNO(I)*(CPE+ZP1+EDN)/DENOM
      TAUX=X+TAUPO(I)*(CNE+ZN1+EDN)/DENOM
      RETURN
C
30    X=TAUNO(I)*ZP1+TAUPO(I)*ZN1
      Y=SQRT(FNC)*SQRT(FNV)*EXP(-EG/(2*CAYT))
      TAUX=1.E30
      IF (Y.EQ.0.) GO TO 40
      TAUX=X/(2*Y)
40    RETURN
C
      END
      SUBROUTINE TAUM(I,CNE,CPE,END,ENA,EDN,TAUX)
C
C   SUBROUTINE TO COMPUTE SPACE-CHARGE NEUTRAL LIFETIMES
C   FOR MULTILEVEL TRAPS
C
C   DESCRIPTION OF ARGUMENTS:
C      I     -  INDEX RANGING FROM 7 TO 10 FOR
C               MULTILEVEL SPECIES.
C      CNE   - THERMAL EQUILIBRIUM DENSITY OF ELECTRONS
C      CPE   - THERMAL EQUILIBRIUM DENSITY OF HOLES
C      END   - POSITION OF THE DONOR TRAP LEVEL
C      ENA   - POSITION OF THE ACCEPTOR TRAP LEVEL
C      EDN   - DENSITY OF EXCESS ELECTRON-HOLE PAIRS
C      TAUX  - COMPUTED VALUE OF THE LIFETIME
C
      DIMENSION NAME1(4),NAME2(4),NAME3(4)
      DIMENSION NAME4(4),NAME5(4),NAME6(4)
      DIMENSION NAME7(4),NAME8(4),NAME9(4),NAME10(4)
      DIMENSION DN(10),DI(10),EN(10),DG(10)
```

```
      DIMENSION SE(10),SH(10)
      DIMENSION TAUNO(10),TAUPO(10)
      COMMON NAME1,NAME2,NAME3,NAME4,NAME5,NAME6
      COMMON NAME7,NAME8,NAME9,NAME10
      CHARACTER*2 NAME1,NAME2,NAME3,NAME4,NAME5,NAME6
      CHARACTER*2 NAME7,NAME8,NAME9,NAME10
      COMMON DN,DI,EN,DG
      COMMON T,CN,CP,EG,FNC,FNV,ALPHA,BETA
      COMMON TAUNO,TAUPO
C
C   COMPUTE GHANDHI'S FACTORS N1 AND P1 CORRECTED FOR DEGENERACY
C
      CAYT=8.6173E-5*T
      ZN1D=FNC*EXP(-(END)/CAYT)/DG(I)
      ZP1D=FNV*EXP(-(EG-END)/CAYT)*DG(I)
      ZN1A=FNC*EXP(-(EG-ENA)/CAYT)*DG(I+1)
      ZP1A=FNV*EXP(-ENA/CAYT)/DG(I+1)
C
C   EVALUATE LIFETIME EXPRESSION
C
      T1=ZN1A*TAUPO(I+1)
      T2=(CPE+EDN)*TAUNO(I+1)
      T3=ZP1D*TAUNO(I)
      T4=(CNE+EDN)*TAUPO(I)
      T5=(CPE+EDN)*TAUNO(I)
      T6=ZN1D*TAUPO(I)
      T7=(CNE+EDN)*TAUPO(I+1)
      T8=ZP1A*TAUNO(I+1)
20    DENOM=(CNE+CPE+EDN)*(T1+T2+T3+T4)
      IF (DENOM.EQ.0.) GO TO 30
      TAUX=((T5+T6)*(T2+T1)+(T4+T3)*(T2+T1)+(T4+T3)*(T7+T8))/DENOM
      RETURN
C
 30   X=T6*T1+T3*T1+T3*T8
      Y=SQRT(FNC)*SQRT(FNV)*EXP(-EG/(2*CAYT))
      TAUX=1.E30
      IF (Y.EQ.0.) GO TO 40
      TAUX=X/(2*Y)/(T1+T3)
40    RETURN
C
      END
```

TABLE D-1. PRINT-OUT OF SAMPLE INPUT TO LIFETIME PROGRAM

```
PHOS        2.0E15   0.045    2.    F
PLAT        2.0E13   0.314    3.7   T
PLAT        2.0E13   0.231    0.5   T


    1.E-16   1.3E-22
    2.E-14    8.E-16
    7.E-15    2.E-14
50.       200.       50.
F
```

TABLE D-2. SAMPLE OUTPUT LISTING FROM LIFETIME PROGRAM

FINDING FERMI LEVEL AT 200. KELVIN

NAME	DENSITY	ENERGY	DEGEN.	CAPTURE CROSS SECTIONS	
				ELECTRON	HOLE
PHOS	2.000E+15	0.0450	2.00	1.0000E-16	1.3000E-22
PLAT	2.000E+13	0.8206	3.70	2.0000E-14	8.0000E-16
PLAT	2.000E+13	0.9036	0.50	7.0000E-15	2.0000E-14

THERMAL EQUILIBRIUM CONDITIONS

TEMP.	1000/T	EF	EG-EF	CARRIER DENSITIES	
				ELECTRON	HOLE
200.000	5.0000	0.9788	0.1557	1.974E+15	1.904E-06

NAME	ION. DEN.	% IONIZED	TAUNO	TAUPO	TAUHIGH
PHOS	1.994E+15	9.968E+01	5.596E-07	3.486E-01	3.486E-01
PLAT	6.020E-07	3.010E-18	2.798E-07	5.665E-06	9.337E-07
PLAT	1.987E+13	9.937E+01	7.994E-07	2.266E-07	9.337E-07

THE HIGH LEVEL TRAP RECOMBINATION LIFETIME IS 9.337E-07 SECONDS

LIFETIME RELATED PARAMETERS

NAME	LOW LEVEL	I.R.=0.01	I.R.=0.10	I.R.=1.00	DEPLETION LAYER
PHOS	1.080E+02	0.000E+00	0.000E+00	0.000E+00	1.733E+12
PLAT	2.280E-07	0.000E+00	0.000E+00	0.000E+00	8.761E-01

LOW LEVEL LIFETIME IS 2.280E-07 SECONDS

LIFETIME IN A DEPLETION LAYER IS 8.761E-01 SECONDS

FEDERAL INFORMATION PROCESSING STANDARD SOFTWARE SUMMARY

01. Summary date: Yr. 84 Mo. 02 Day 14

02. Summary prepared by *(Name and Phone)*: J. R. Lowney and W. R. Thurber, (301) 921-3625

03. Summary action: New [X] Replacement [ ] Deletion [ ]
Previous Internal Software ID:

04. Software date: Yr. Mo. Day

05. Software title: A FORTRAN Program for Calculating the Recombination Lifetime of Silicon

06. Short title: Lifetime-Predicting Computer Program (LT1)

07. Internal Software ID:

08. Software type:
- [ ] Automated Data System
- [X] Computer Program
- [ ] Subroutine/Module

09. Processing mode:
- [ ] Interactive
- [ ] Batch
- [X] Combination

10. Application area

General:
- [ ] Computer Systems Support/Utility
- [X] Scientific/Engineering
- [ ] Bibliographic/Textual
- [ ] Management/Business
- [ ] Process Control
- [ ] Other

Specific: Engineering calculation

11. Submitting organization and address:
National Bureau of Standards
Semiconductor Materials & Processes Division
Bldg. 225, Rm. A331
Washington, DC 20234

12. Technical contact(s) and phone:
J. R. Lowney (301) 921-3625
W. R. Thurber (301) 921-3625
R. D. Larrabee (301) 921-3625

13. Narrative:
This computer program computes the recombination lifetime in silicon due to traps as a function of temperature and carrier density. The trap energy, density, and cross sections are needed as input for each deep level present. Shockley-Read-Hall theory is used with provision made for multiple species.

14. Keywords:
Computer program; deep level; injection ratio; recombination lifetime; silicon; trap

15. Computer manuf'r and model	16. Computer operating system	17. Programing language(s)	18. Number of source program statements
Univac 1100	Exec 9R1	FORTRAN-77	1,000

19. Computer memory requirements	20. Tape drives	21. Disk/Drum units	22. Terminals
60K	none	none	printer

23. Other operational requirements:
None

24. Software availability:
Available [X] Limited [ ] In-house only [ ]

See item 12 for contacts.

25. Documentation availability:
Available [X] Inadequate [ ] In-house only [ ]

1. See item 12 for contacts.
2. See NBSIR 84-2838

26. FOR SUBMITTING ORGANIZATION USE

Standard Form 185
1974 July
U.S. Dept. of Commerce—NBS
(FIPS Pub 30)

NBS-114A (REV. 2-8C)

U.S. DEPT. OF COMM. BIBLIOGRAPHIC DATA SHEET (See instructions)	1. PUBLICATION OR REPORT NO. NBSIR 84-2838	2. Performing Organ. Report No.	3. Publication Date April 1984

4. TITLE AND SUBTITLE

Measurement Techniques for High Power Semiconductor Materials and Devices: Annual Report, January 1, 1982 to March 31, 1983

5. AUTHOR(S)

W. R. Thurber, J. R. Lowney, and W. E. Phillips

6. PERFORMING ORGANIZATION (If joint or other than NBS, see instructions)

NATIONAL BUREAU OF STANDARDS
DEPARTMENT OF COMMERCE
WASHINGTON, D.C. 20234

7. Contract/Grant No.
NBS/DOE DE-A101-76PR06010

8. Type of Report & Period Covered
Final
1/1/82 to 3/31/83

9. SPONSORING ORGANIZATION NAME AND COMPLETE ADDRESS (Street, City, State, ZIP)

Department of Energy
Division of Electric Energy Systems
Washington, DC 20461

10. SUPPLEMENTARY NOTES

[X] Document describes a computer program; SF-185, FIPS Software Summary, is attached.

11. ABSTRACT (A 200-word or less factual summary of most significant information. If document includes a significant bibliography or literature survey, mention it here)

This annual report is the final one in a series which describes NBS research to develop procedures for the effective utilization of deep-level measurements to detect and characterize defects which reduce lifetime or contribute to leakage current in power-device-grade silicon. During this reporting period the previously written computer program for predicting excess-carrier lifetime was revised to calculate more accurately lifetimes for high or low injection conditions and in space-charge regions. Comparisons were made between lifetime measurements on platinum-doped silicon diodes and the predictions of the computer model. As part of the effort to extend the procedures to analyze data from nonexponential transient capacitance measurements, the time dependence of the capacitance-voltage relationship of a heavily platinum-doped silicon diode was measured as a function of bias voltage. Included as appendices are three recent publications resulting from the work. A listing of the lifetime-predicting computer program is also an appendix.

12. KEY WORDS (Six to twelve entries; alphabetical order; capitalize only proper names; and separate key words by semicolons)

Deep-level measurements; deep-level transient spectroscopy; defect characterization; lifetime; power-device grade silicon; transient capacitance techniques.

13. AVAILABILITY

[X] Unlimited
[ ] For Official Distribution. Do Not Release to NTIS
[ ] Order From Superintendent of Documents, U.S. Government Printing Office, Washington, D.C. 20402.
[X] Order From National Technical Information Service (NTIS), Springfield, VA. 22161

14. NO. OF PRINTED PAGES
52

15. Price
$10.00